

Contents lists available at [ScienceDirect](http://www.sciencedirect.com)

European Economic Review

journal homepage: www.elsevier.com/locate/euroecorev

Climate change policy under polar amplification☆☆☆

W. Brock^{a,b}, A. Xepapadeas^{c,d,*}^a Economics Department, University of Wisconsin, United States^b University of Missouri, USA^c Department of International and European Economic Studies, Athens University of Economics and Business, Greece^d Department of Economics, University of Bologna, Italy

ARTICLE INFO

Article history:

Received 2 June 2016

Accepted 9 March 2017

Available online 27 June 2017

JEL Classification:

Q54

Q58

Keywords:

Polar amplification

Spatial heat and moisture transport

Optimal policy

Emission taxes

Market discount rate

ABSTRACT

Polar amplification is an established scientific fact which has been associated with the surface albedo feedback and with heat and moisture transport from the Equator to the Poles. In this paper we unify a two-box climate model, which allows for heat and moisture transport from the southern region to the northern region, with an economic model of welfare optimization. Our main contribution is to show that by ignoring spatial heat and moisture transport and the resulting polar amplification, the regulator may overestimate or underestimate the tax on greenhouse gas emissions. The direction of bias depends on the relations between marginal damages from temperature increase in each region. We also determine the welfare cost when a regulator mistakenly ignores polar amplification. Numerical simulations confirm our theoretical results, while ballpark estimates indicate that the tax bias could be as high as 20%, while welfare cost could reach 2% of global effective steady-state consumption.

© 2017 Elsevier B.V. All rights reserved.

1. Introduction

A well-established fact in the science of climate change is that when the climate cools or warms, high latitude regions tend to exaggerate the changes seen at lower latitudes. This effect is called polar amplification (PA). According to the *IPCC* (2013, p. 396):

“Polar amplification occurs if the magnitude of zonally averaged surface temperature change at high latitudes exceeds the globally averaged temperature change, in response to climate forcings and on time scales greater than the annual cycle.”

PA is a global concern because of its possible future effects on ice sheet stability and the related consequences. Recent studies indicate the magnitude of PA. *Bekryaev et al. (2010)*, using an extensive data set of monthly surface air temperature, documents a high-latitude (>60°N) warming rate of 1.36°C/century for 1875–2008, with the trend being almost two times stronger than the Northern Hemisphere trend of 0.79°C/century. The high-latitude warming rate accelerated in the most recent decade to 1.35°C/decade which is a manifestation of PA. *Winton (2006)* reports a mean annual Arctic (60° N–90° N) warming that is, on average, 1.9 times greater than the global mean warming at the time of carbon dioxide doubling. Similar

* We are grateful to the editors and two anonymous reviewers for valuable comments and suggestions on earlier drafts of this paper.

☆☆ A Publisher's error resulted in this article appearing in the wrong issue. This article is reprinted here for the reader's convenience and for the continuity of the Special Issue. For citation purposes, please use the original publication details; *Eur. Econ. Rev.*, 94, 263–282. DOI of original item: <http://dx.doi.org/10.1016/j.euroecorev.2017.03.003>. Copyright line should match previous version-002, 2017.

* Corresponding author at: Department of International and European Economic Studies, Athens University of Economics and Business, Greece.

E-mail addresses: wbrock@ssc.wisc.edu (W. Brock), xepapad@aub.gr, xepapad@gmail.com (A. Xepapadeas).

results for PA are reported by [Serreze and Barry \(2011\)](#) who point out that special attention should be given to the Arctic Ocean where the strongest amplification is expected to occur. The phenomenon of PA has therefore been well-established in the Northern Hemisphere, and is referred to as Arctic Amplification (AA). At the same time, most modern climate models project that increases in Antarctic temperature through the 21st century will be smaller than those in the Arctic, due to the very different geography of Antarctica (see [Pithan and Mauritsen, 2014](#); [Serreze and Barry, 2011](#); [Stroeve et al., 2007](#), Fig. 1).

Regarding the mechanism causing AA, the discussion was initially focused on the surface-albedo feedback (SAF) which can be traced back to [Arrhenius \(1897\)](#). The SAF mechanism suggests that initial warming in the North Pole will melt some of the Arctic's highly reflective (high albedo) snow and ice cover. This will expose darker surfaces which will absorb solar energy, leading to further warming and further retreat of snow and ice cover. However, recent literature provides a variety of mechanisms other than SAF which can cause PA (see for example [Graversen and Wang, 2009](#); [Pithan and Mauritsen, 2014](#); [Serreze and Barry, 2011](#)). One of these mechanisms resulting from experiments undertaken by [Alexeev \(2003\)](#) and [Alexeev et al. \(2005\)](#) with an aqua-planet model without sea-ice and land-ice, and therefore without SAF, revealed that PA emerges as a result of an increase in the meridional heat transport. [Langen and Alexeev \(2007\)](#) interpreted PA as an inherent dynamical property of the system.

However, although PA is regarded by climate science as a near universal feature of climate model simulations of the planet's response to increasing atmospheric greenhouse gas (GHG) concentrations (e.g., [Serreze and Barry, 2011](#)),¹ this feature has been largely ignored by the economics of climate science. As pointed out by [Dietz and Stern \(2015\)](#), the science of climate change has been running years ahead of the economics of climate change. [Moyer et al. \(2014\)](#) made a similar point earlier and also stressed the importance of growth effects as well as level effects of climate change damages. The purpose of this paper is, therefore, to introduce PA and spatial heat transport into an economic model of climate change and explore their impacts on the design of climate policy in the form of carbon taxes. In this context, the present paper can be seen as extending the literature on the optimal taxation of GHG emissions by accounting for the PA effect, which is modelled by using a two-box model representing the heat transport from the Equator to the Poles. In the model, box 2 represents the higher latitudes (30–90°N) and box 1 the lower latitudes (0–30°N). This model is coupled with a simple welfare-maximization problem to derive the optimal GHG emission path in the two regions. The model we use is based on the two-box models of the meridional heat transport mechanism developed by [Alexeev \(2003\)](#), [Alexeev et al. \(2005\)](#), and [Alexeev and Jackson \(2013a, 2013b\)](#). Such models present mechanisms of heat transport, polar magnification, and ice line movement effects due to outside forcing along with a simple treatment of moisture transport.²

Three reservoir (or box) models describing the carbon cycle have been used in the economics of climate change (e.g. [Gerlagh and Liski, 2016](#); [Golosov et al., 2014](#); [Nordhaus and Sztorc, 2013](#)). In this paper, what we refer to as a two-box model is a model where boxes represent two geographical regions with heat and moisture transport from the low latitude region to the high latitude region. We keep the “two-box” terminology, following [Alexeev \(2003\)](#), but we emphasize that boxes refer to geographic regions and not to boxes or reservoirs for carbon diffusion. Four-box ocean models have been used to study emissions and abatement paths associated with a potential tipping point of the Atlantic thermohaline circulation (see [Belaia et al., 2015](#); [Zickfeld and Bruckner, 2008](#); [Zickfeld et al., 2004](#)). Our simplified two-box model does not include ocean boxes but allows us to study the link between damages and local temperatures and to characterize biases and welfare loss from ignoring PA when policy is designed.

In particular, if we denote the temperature anomaly – that is, the change in temperature relative to a given benchmark temperature – in each box or region by T_1 and T_2 respectively, the relaxation time of the box anomaly temperature gradient, $T_1 - T_2$, is faster than the relaxation time of the box anomaly global mean temperature, $(T_1 + T_2)/2$ ([Langen and Alexeev, 2007](#), Eq. (23)). This difference is important in terms of economics since it is related to damages associated with temperature differences across different latitudes, in contrast to damages related to the planetary global average temperature. Therefore PA, apart from its importance for climate science, is also important for the economics of climate change and in particular the characterization of local damages and local policies.

We now briefly discuss costs and benefits associated with PA, in order to provide a clear picture of their importance. AA causes loss of Arctic sea ice which in turn has consequences for melting land ice along with other effects. According to the [IPCC \(2013, p. 9\)](#):

“The annual mean Arctic sea ice extent decreased over the period 1979–2012 with a rate that was very likely in the range 3.5–4.1% per decade (range of 0.45–0.51 million km² per decade), and very likely in the range 9.4–13.6% per decade (range of 0.73–1.07 million km² per decade) for the summer sea ice minimum (perennial sea ice). There is medium confidence from reconstructions that over the past three decades, Arctic summer sea ice retreat was unprecedented.”

¹ As [Langen and Alexeev \(2007\)](#) indicate, PA is seen in model projections of future climate (e.g., [ACIA, 2004](#); [Holland and Bitz, 2003](#)) and, in fact, in the very earliest simple model of CO₂-induced climate change ([Arrhenius, 1897](#)). PA is found in proxy-records of both deep past warm periods (e.g., [Zachos et al., 2001](#)) and of the more recent cold glacials (e.g., [Masson-Delmotte et al., 2006](#)).

² [Brock et al. \(2013, 2014b\)](#) use a more realistic energy balance model because it models the Earth by a continuum of latitudes and considers heat transport across latitudes, i.e., it has a “continuum of boxes” with heat transport across each. However, more advanced mathematics is required for this analysis.

Sea ice loss in the summer will generate a positive feedback to AA since it will lead to thinner ice in the winter, more sea ice loss in the following summer and so on [Serreze and Barry \(2011\)](#). AA and ice loss is expected to increase the frequency of extreme weather events in the Northern Hemisphere ([Francis and Skific, 2015](#); [Francis and Vavrus, 2014](#)).

Melting land ice associated with a potential meltdown of Greenland and West Antarctica ice sheets due to PA might cause serious global sea level rise. It is estimated that the ice sheets in Greenland and West Antarctica hold an equivalent of 2–7 m and 5 m of global sea level rise respectively (see [Lenton et al., 2008](#)). Recent projections suggest that irreversible melting of the Greenland ice sheet could be triggered during this century ([IPCC, 2013](#)).³

Another source of damages caused by PA relates to the thawing of permafrost, which is soil at or below the freezing point of water (0°C or 32° F) for two or more years. Permafrost regions occupy approximately 22.79 million km² (about 24% of the exposed land surface) of the Northern Hemisphere ([Zhang et al., 2003](#)). The [IPCC \(2013, p. 9\)](#) states that:

“There is high confidence that permafrost temperatures have increased in most regions since the early 1980s. Observed warming was up to 3° C in parts of Northern Alaska (early 1980s to mid-2000s) and up to 2° C in parts of the Russian European North (1971–2010).

Recent work investigating the permafrost carbon pool size estimates that 1400–1700 Gt of carbon is stored in permafrost soils worldwide. This large carbon pool represents more carbon than currently exists in all living things and twice as much carbon as exists in the atmosphere ([Tarnocai et al., 2009](#)). Thawing of permafrost caused by PA is expected to bring widespread changes in ecosystems, increase erosion, harm subsistence livelihoods, and damage buildings, roads, and other infrastructure (see for example [Schaefer et al., 2014](#); [Schuur et al., 2015](#)). Loss of permafrost will also cause release of GHGs with global effects. The [IPCC \(2013\)](#) assesses that the release of CO₂ or CH₄ into the atmosphere from thawing permafrost carbon stocks over the 21st century will be in the range of 50–250 GtC for the Representative Concentration Pathway 8.5. Issues such as melting of land ice or thawing of permafrost therefore suggest that PA might be an important factor in the effort to design efficient climate policies.⁴

On the other hand, according to [Borgerson \(2008\)](#), the loss of sea ice due to AA may generate economic benefits which include increased access to Arctic fish, timber, and minerals such as lead, magnesium, nickel and zinc, along with immense freshwater reserves, which could become increasingly valuable, unexplored hydrocarbon reserves, and opening of new sea routes in the North. These benefits are not, however, free of potential costs, since access to resources might also generate political conflicts as nearby countries will compete for their share ([Borgerson, 2008](#)).

The above discussion suggests that AA could be a source of damages to midlatitudes through extreme weather events, sea level rise, permafrost feedbacks and political conflicts, but also a source of potential benefits. Although exact damages seem uncertain, they could become large in the future and in fact may already be large (see for example [Kug et al., 2015](#); [Rahmstorf and Coumou, 2011](#); [Screen and Simmonds, 2014](#)).

In this context our paper seeks to provide new insights into the economics of climate change by incorporating PA into economic modeling. Using the two-box model we accomplish four tasks which represent the contributions of this work.

First, the optimal carbon tax is computed and then compared with the tax resulting from a version of the model in which heat transport is ignored by the decision maker. The bias in the tax is then shown to depend on the regional damage shares and the basic parameters of the PA effect. The directionality of heat energy and moisture transport - from the lower latitudes to the higher latitudes - interacting with the pattern of relative marginal damages from temperature increases across latitudes determines the bias in optimal carbon taxes. We create a “how much spatial heat transport matters index” by taking the ratio of the value of the optimal carbon tax when there is spatial heat transport to the value of the tax when spatial transport is zero. We show that “space matters” when the high latitude share of marginal damages deviates from $\frac{1}{2}$. More specifically, when heat transport from lower to higher latitudes is associated with higher marginal damages to both regions from a temperature increase in the North than in the South, our ballpark estimates indicate that the tax bias could be between 6% and 20%. While we are able to use theory to isolate potential directions and strengths of these biases, and to make plausible qualitative statements about their potential sizes, serious calibration and computational work is needed to obtain quantitative estimates. This is beyond the scope of this article. We would also like to emphasize that our results should be interpreted as indicative of biases in the recommended carbon taxes and the welfare effects of climate change which emerge if heat and moisture transport is not properly accounted for in Integrated Assessment Modeling.⁵

In relation to existing literature on carbon taxes with spatial structure, [D’Autume et al. \(2016\)](#) study carbon taxation in second best frameworks as well as settings in which lump sum compensatory transfers are and are not possible. They locate a set of sufficient conditions for carbon taxes to be uniform across locations, especially if lump sum compensatory transfers are available. However, under the realistic political constraints on transferring resources across countries, they find

³ See also the burning embers diagram for the likelihood of tipping of Greenland and West Antarctica ice-sheets under different degrees of global warming in [Lenton \(n.d.\)](#).

⁴ Melting of land ice and permafrost thawing are related to the concept of damage reservoirs (see [Brock et al., 2014a](#)).

⁵ [Cai et al. \(2017\)](#) include spatial transport of heat and moisture from the Equator to the Poles in an extension of the stochastic DSICE model of [Cai et al. \(2015b, 2015a\)](#) in order to study the impacts of PA on the optimal paths of key quantities like the Social Cost of Carbon (SCC), emissions, abatement, and damages. The numerical solution of this model requires the use of blue waters super computer technology. This approach uses realistic time/quantity scales, but on the other hand insights into what is driving the findings and what is driving the direction of the biases are hard to identify. The simple model we develop here is very useful in attaining this objective.

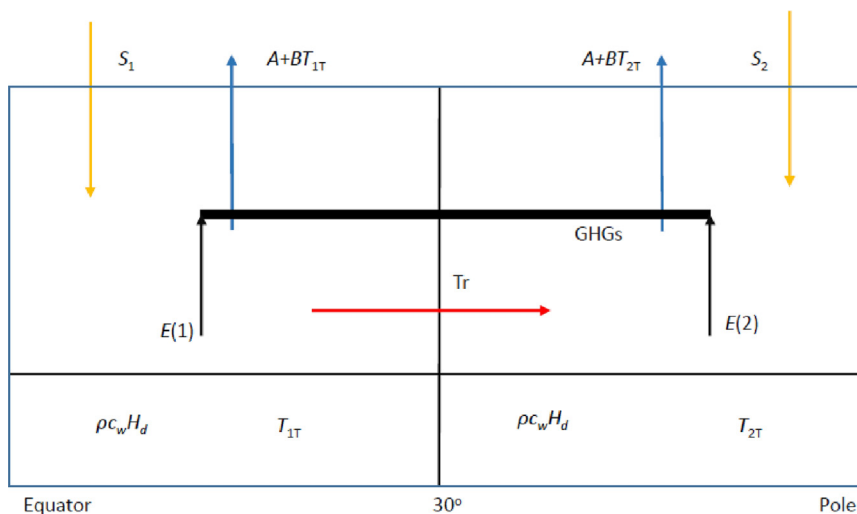


Fig. 1. The two-box energy balance model.

that equity concerns force carbon taxes to be lower for poorer areas. Brock et al. (2013) and Brock et al. (2014b), in a model of continuous space that allows for spatial heat transport, show that externality taxes (i.e. carbon prices) should be uniform when compensatory transfers are possible, but tend to be lower in poorer areas when such transfers are not available. They do not, however, analytically characterize the bias in taxes, due to the complexity of the continuous-space dynamical models, or the welfare cost from ignoring heat and moisture transfer. We consider this to be a major advantage of the two-box model approach.

Second, in addition to the calculation of optimal taxes, the welfare costs are computed of having wrong beliefs about the parameters characterizing PA because a regulator believes that the parameters of the climate system are such that PA is not present. We consider this calculation necessary because the qualitative analysis to reveal the potential bias on carbon taxes from ignoring the PA effect does not reveal the corresponding welfare impact. We also show that this welfare impact, measured in steady-state effective consumption terms, could be significant.

The rest of the paper is structured as follows. Section 2 presents the two-box model, Section 3 derives optimal carbon taxes and the bias from ignoring PA, and Section 4 shows how to calculate the welfare cost when PA is ignored. Section 5 concludes. Proofs and derivations are provided in an appendix.

2. A two-box energy balance model with anthropogenic emissions of greenhouse gasses

The two-box energy balance model introduced by Langen and Alexeev (2007) and Alexeev and Jackson (2013a) consists of a single hemisphere with two boxes or regions divided by the 30th latitude, which yields similar surface area of the two boxes. Following Langen and Alexeev (2007), the two-box model is presented below.

In Fig. 1, T_{xT} , $x = 1, 2$ is the ocean mixed-layer temperatures in each box, with 1 denoting the lower latitude and 2 the higher latitude. This temperature is defined as the sum of equilibrium, or baseline, average temperature in each box (T_{1b} , T_{2b}) when anthropogenic forcing through emissions of GHGs is zero, plus the temperature anomaly (T_1 , T_2). Thus $T_x = T_{xT} - T_{xb}$, $x = 1, 2$. By the definition of the boxes (or regions), the baseline average yearly temperatures (T_{1b} , T_{2b}) satisfy the inequality $T_{1b} > T_{2b}$. The downwelling short wave radiation in each region is denoted by S_x , the outgoing longwave radiation by $A + BT_{xT}$, the heat transport from box 1 to box 2 by Tr and the stock of GHGs created by anthropogenic emissions by GHG . This stock traps part of the outgoing longwave radiation. In the two-box model the ocean mixed layer has in both boxes a depth of H_d , density ρ_d , and heat capacity c_w , thus we denote by $H = \pi a_e^2 \rho_d c_w H_d$ the upper ocean layer heat capacity, where a_e is the radius of the Earth and πa_e^2 yields half the area of the hemisphere. Assuming no anthropogenic forcing, the evolution of the ocean mixed-layer temperature in each box is:

$$\dot{T}_{1T} = \frac{1}{H} (S_1 - A - BT_{1T} - Tr) \quad (1)$$

$$\dot{T}_{2T} = \frac{1}{H} (S_2 - A - BT_{2T} + Tr). \quad (2)$$

The meridional heat transport is defined in terms of the temperature anomaly as:

$$Tr = \bar{Tr} + \gamma_1 (T_1 - T_2) + \gamma_2 T_1. \quad (3)$$

In (3) the first term, $\bar{T}r$, is the equilibrium heat transport, the second term captures the increase in transport due to increasing baroclinicity, while the third term captures the effect of an increased moisture supply and thus greater latent heat transport with increased low- to mid-latitude temperatures. In the dynamical system (1) and (2), we use the parameterization of Alexeev et al. (2005) and add the anthropogenic impact of GHG emissions.

To model the impact of carbon emissions on temperature, we follow Matthews et al. (2009) and MacDougall and Friedlingstein (2015) and use an approximately constant transient climate response to cumulative CO₂ emissions (TCRE), Λ , defined as $\Lambda = \frac{\Delta T(t)}{CE(t)}$, where $CE(t)$ denotes cumulative carbon emissions up to time t and ΔT the change in temperature during the same period. The constancy of Λ suggests a linear relationship between a change of global average temperature and cumulative emissions. This linear relationship (see Matthews et al., 2009; 2012) has also been recognized by the IPCC (2013),⁶ while in the same context Knutti (2013) concludes that every ton of CO₂ causes about the same amount of warming, no matter when and where it is emitted. The linear relationship between a change of global average temperature and cumulative emissions is discussed in more detail in Appendix A.⁷

In the context of the near proportional relationship between $CE(t)$ and $\Delta T(t)$, the anthropogenic impact on the global temperature increase can be approximated in continuous time by $T(t) - T(0) = \Lambda \int_{s=0}^t E(s)ds$, where $CE(t) = \int_{s=0}^t E(s)ds$ denotes cumulative global carbon emissions up to time t and Λ is the TCRE. Taking the time derivative of (A.4), we obtain

$$\dot{T}(t) = \Lambda E(t). \tag{4}$$

We consider this continuous time approximation as a useful short cut, which is supported by climate science, so that simple optimal control theory can be used to provide insights and suggest the direction of biases when PA is ignored. Thus our abstraction using $\dot{T}(t) = \Lambda E(t)$ allows the use of simple mathematical modeling in a two-box model. Note that the two-box model is also an abstraction which is, however, very helpful in providing insights about the mechanisms driving PA.

In our two-box model, global emissions at each date t are defined as the sum of emissions in box 1, $E(1, t)$, and box 2, $E(2, t)$, or $E(t) = E(1, t) + E(2, t)$. It should be noted that these emissions can also be interpreted by an appropriate choice of units as fossil fuel use. Under the linear approximation of the anthropogenic impact, the dynamical system (1) and (2) can be expressed in terms of the evolution of the temperature anomaly in each box as:

$$\dot{T}_1 = \frac{1}{H} [(-B - \gamma_1 - \gamma_2)T_1 + \gamma_1 T_2 + \Lambda E(t)], \quad T_1(0) = 0 \tag{5}$$

$$\dot{T}_2 = \frac{1}{H} [(\gamma_1 + \gamma_2)T_1 + (-B - \gamma_1)T_2 + \Lambda E(t)], \quad T_2(0) = 0 \tag{6}$$

$$E(t) = E(1, t) + E(2, t). \tag{7}$$

Suppose, for the moment, that $E(t)$ is constant so a steady state exists for (5)–(7). It can easily be seen from (5)–(7) that when $\gamma_2 = 0$, the steady-state temperature anomaly between low and high latitudes is the same, and that the ratio between low latitude warming and high latitude warming is one. On the other hand, in a steady state where $\gamma_2 > 0$, the ratio is greater than one. Thus the term $\gamma_2 T_1$ in (3) breaks symmetry between the two boxes if $E(t)$ is constant. Of course $E(t)$ is not constant, but this is enough to make our point about symmetry breaking. In Section 3 $E(t)$ is a choice variable in the optimization problem.

While the model (1) and (2) strictly represents a form of PA based on changes in the meridional heat transport (Langen and Alexeev, 2007, p. 309), the SAF is also regarded as an important PA mechanism, as mentioned in the introduction. The SAF mechanism, which along with tipping points could introduce nonlinearities, is not captured by (5)–(7), however, this model can be easily modified to allow for a simple linear SAF mechanism. Our conjecture, presented in Appendix B, is that with the SAF effect added, the box 2 temperature will be higher and thus any damage flow towards box 1 caused by higher temperature in box 2 will be increased.

⁶ In IPCC (2013, p. 1113), it is stated that:

In conclusion, taking into account the available information from multiple lines of evidence (observations, models and process understanding), the near linear relationship between cumulative CO₂ emissions and peak global mean temperature is well established in the literature and robust for cumulative total CO₂ emissions up to about 2000 PgC. It is consistent with the relationship inferred from past cumulative CO₂ emissions and observed warming, is supported by process understanding of the carbon cycle and global energy balance, and emerges as a robust result from the entire hierarchy of models.

⁷ Leduc et al. (2015, 2016) discuss the limits of the approximation and Leduc et al. (2016) show that it also holds at the regional level although, as they point out, the linear approximation is rather crude, especially in the higher latitudes.

3. Social welfare optimization and optimal carbon tax under polar amplification

To study optimal climate policy in the context of the two-box climate model described above, we consider a simple welfare maximization problem with logarithmic utility, where world welfare is expressed by the sum of welfare in each region and is given by:

$$\int_{t=0}^{\infty} e^{-\rho t} \left[\sum_{x=1}^{x=2} v(x) L(x, t) \ln[y(x, t) E(x, t)^{\alpha} e^{-\phi(x, T_b+T)}] \right] dt, \quad (8)$$

where $y(x, t)E(x, t)^{\alpha}$, $0 < \alpha < 1$, $E(x, t)$, $T_{ib}(x, t)$, $T_i(x, t)$, $L(x, t)$ are output per capita, fossil fuel input or emissions of GHGs, baseline temperature, temperature anomaly, and fully employed population in each region x at date t , respectively. We follow Golosov et al. (2014) and assume exponential damages.⁸ Thus the term $e^{-\phi(x, T_b+T)}$, $T_b + T = (T_{1b} + T_1, T_{2b} + T_2)$ reflects damages to output per capita in region $x = 1, 2$ from an increase in the temperature anomaly in either region, since PA in region 2 might generate damages to region 1. We assume that $y(x, t)$, $L(x, t)$ are exogenously given. That is, we are abstracting away from the problem of optimally accumulating capital inputs and other inputs in order to focus sharply on optimal fossil fuel taxes. In this context $y(x, t)$ could be interpreted as the component of a Cobb–Douglas production function that embodies all other inputs along with technical change that evolves exogenously. Finally, $v(x)$ represents welfare weights associated with box (or region) x . We emphasize that our model is a stylized two-region model, specially designed to focus on sharply exposing the forces of heat and moisture transport from the low latitude region of the Northern Hemisphere towards the North Pole of the high latitude region of the Northern Hemisphere and, by necessity some important economics is left out⁹ in order to more clearly reveal the influence of heat and moisture transport.¹⁰

Assuming that each region has its own fossil fuels reserves, denoted by $R_0(x)$, the resource constraint for each region becomes:

$$\int_{t=0}^{\infty} E(x, t) dt \leq R_0(x), \quad x = 1, 2. \quad (9)$$

The welfare optimization problem is, therefore, to choose the fossil fuel (or GHG emissions) path to maximize (8) subject to (5)–(7) and (9).¹¹ To simplify and allow study of the property of optimal steady states, we assume that $L(x, t) = L(x)$, $y(x, t) = y(x)$, $x = 1, 2$ for all dates.¹² Dropping the term $v(x)L(x, t)\ln y(x, t)$, which does not affect optimality conditions, the current value Hamiltonian function for the welfare maximization problem becomes:

$$\begin{aligned} \mathcal{H} = & \sum_{x=1}^{x=2} \left\{ v(x)L(x) [\alpha \ln E(x, t) - \phi(x, T_b + T)] - \Lambda_{R_0^x} E(x, t) \right\} \\ & + \Lambda_{T_1} \frac{1}{H} [(-B - \gamma_1 - \gamma_2)T_1 + \gamma_1 T_2 + \Lambda[E(1, t) + E(2, t)]] \\ & + \Lambda_{T_2} \frac{1}{H} [(\gamma_1 + \gamma_2)T_1 + (-B - \gamma_1)T_2 + \Lambda[E(1, t) + E(2, t)]] \\ & T_b = (T_{1b}, T_{2b}), \quad T = (T_1, T_2). \end{aligned} \quad (10)$$

The following first-order necessary conditions (FONC) for the optimal choice of fossil fuel (or emissions) use can be obtained by differentiating the Hamiltonian w.r.t. $E(x, t)$,

$$\frac{\alpha v(x)L(x)}{E(x, t)} = \frac{-\Lambda(\sum_{i=1}^2 \Lambda_{T_i}(t))}{H} + \Lambda_{R_0^x}(t), \quad \text{or} \quad (11)$$

$$E(x, t) = \frac{-\alpha v(x)L(x)H}{[-\Lambda(\sum_{i=1}^2 \Lambda_{T_i}(t)) + \Lambda_{R_0^x}(t)]}, \quad x = 1, 2. \quad (12)$$

If we assume that both regions share the total initial fossil fuel reserves, then resource constraints (9) should be replaced by the single constraint

$$\int_{t=0}^{\infty} E(t) dt = \int_{t=0}^{\infty} \sum_{x=1}^{x=2} E(x, t) dt \leq R_0, \quad R_0 = R_0(1) + R_0(2). \quad (13)$$

⁸ A large body of research in climate change economics assumes that damages are not exponential (e.g., Nordhaus and Sztorc, 2013; Weitzman, 2010). We use exponential damages for the same tractability reasons as in Golosov et al. (2014).

⁹ For example, we assume fixed initial fossil fuel reserves when they are evidently not fixed (e.g., shale gas). Furthermore the model has full exhaustion of reserves. For a more realistic, but computationally intensive model, see Cai et al. (2017).

¹⁰ We focus on the Northern Hemisphere because the geography is very different at the Southern Hemisphere, the PA is weaker there and, most importantly, most of the world's economic activity takes place North of the Equator. Evidence indicates that 88% of the global population lives in the Northern Hemisphere (<http://www.radicalcartography.net/index.html?histpop>).

¹¹ Problem (8) refers to a cooperative solution. An interesting area for further research would be the study of non-cooperative Nash outcomes, either open or closed-loop.

¹² We could also have assumed that L and y grow exponentially and have their growth rates absorbed into the utility discount rate.

Then the multipliers $\Lambda_{R_0^x}(t)$ should be replaced by the single multiplier $\Lambda_{R_0}(t)$ in the FONC (11).

It can be seen from (11) that the externality tax associated with anthropogenic emissions of GHGs – the optimal carbon tax – is:

$$\tau(t) = \frac{-\Lambda(\sum_{i=1}^2 \Lambda_{T_i}(t))}{H}. \tag{14}$$

Note that the externality tax is likely to increase as the cumulative carbon response parameter, Λ , of Matthews et al. (2009) increases and the heat capacity H decreases. Of course, in order to characterize the optimal carbon tax, the paths of the regional temperature costates, $(\Lambda_{T_1}(t), \Lambda_{T_2}(t))$, which reflect the regional shadow cost from a temperature increase, should be taken into account in order to obtain the total effect on the externality tax. Under our simplifying assumptions to be stated below, τ is a useful “sufficient parameter” for all the quantities that are policy-relevant. That is, the emissions at each set of latitude belts, $x = 1, 2$; the optimal “price” path of reserves, $R_0(x)$; and optimal welfare are all functions of τ .

Furthermore if fossil fuel reserves plus anticipated new discoveries in each region are infinite, then $\Lambda_{R_0^x}(t) = 0$ for all dates t , and $x = 1, 2$ or $\Lambda_{R_0}(t) = 0$ for all dates t , if we consider the case in which the two regions share infinite reserves. If the reserves are finite, then their shadow price Λ_{R_0} rises at rate ρ over time. When the initial reserve plus anticipated new discoveries is finite, the initial value $\Lambda_{R_0}(0)$ is set by the resource constraints,

$$\int_{t=0}^{\infty} E(x, t) dt = R_0(x), \quad x = 1, 2, \quad \text{or} \quad \int_{t=0}^{\infty} \sum_{x=1}^{x=2} E(x, t) dt = R_0. \tag{15}$$

In order to obtain some straightforward insights about the interaction of climate and economics in the simplest possible setting, we restrict ourselves to the case in which $\frac{\partial \phi(x, T_b + T)}{\partial T_i}$ is constant for all $x = 1, 2$ and $i = 1, 2$.

Assumption 1. Define marginal damage cost of temperature increase in box $x = 1, 2$ by

$$d_i = d_{1i} + d_{2i} = \sum_{x=1}^{x=2} v(x)L(x) \frac{\partial \phi(x, T_b + T)}{\partial T_i}, \quad i = 1, 2, \tag{16}$$

where

$$v(1)L(1)\phi(1, T_b + T) = d_{11}(T_{1b} + T_1) + d_{12}(T_{2b} + T_2) \tag{17}$$

$$v(2)L(2)\phi(2, T_b + T) = d_{21}(T_{1b} + T_1) + d_{22}(T_{2b} + T_2). \tag{18}$$

We assume that $d_i, i = 1, 2$ are constants at all dates.

In Assumption 1 the parameters (d_{12}, d_{21}) capture the cross effects from an increase in the temperature anomaly in one region on the damages of the other region. In particular, d_{12} captures the effects of PA in region 2 on damages in region 1. Thus $d_1 = d_{11} + d_{21}$ is the aggregate impact (i.e. the impact on both regions) from a temperature increase in region 1, while $d_2 = (d_{12} + d_{22})$ is the aggregate impact from a temperature increase in region 2. If we assume that the PA effects on region 1 are sufficiently strong, and d_{21} is negligible, then $d_2 > d_1$ might reflect strong PA effects.

Setting $H = 1$ to ease notation,¹³ the optimality conditions for costate equations of the climate dynamics of (10) imply the following dynamic linear system:

$$\dot{\Lambda}_{T_1} = [\rho + (B + \gamma_1 + \gamma_2)]\Lambda_{T_1} - (\gamma_1 + \gamma_2)\Lambda_{T_2} + d_1 \tag{19}$$

$$\dot{\Lambda}_{T_2} = -\gamma_1 \Lambda_{T_1} + [\rho + (B + \gamma_1)]\Lambda_{T_2} + d_2. \tag{20}$$

It is straightforward to see that the optimal solutions for the costates are the steady-state values for the costates obtained by setting $(\dot{\Lambda}_{T_1}, \dot{\Lambda}_{T_2}) = (0, 0)$, or

$$\Lambda_{T_1} = -(\beta d_1 + \gamma_1 d_2 + \gamma_2 d_2) / \Gamma \tag{21}$$

$$\Lambda_{T_2} = -(\beta d_2 + \gamma_2 d_2 + \gamma_1 d_1) / \Gamma \tag{22}$$

$$\beta = \rho + (B + \gamma_1), \quad \Gamma = \beta^2 - (\gamma_1)^2 + \beta \gamma_2 - \gamma_1 \gamma_2. \tag{23}$$

Then, steady-state optimal carbon tax is defined as

$$\tau = -\Lambda(\Lambda_{T_1} + \Lambda_{T_2}). \tag{24}$$

¹³ Setting $H = 1$ just amounts to absorbing H into the parameters $\lambda, B, \gamma_1, \gamma_2$ because it always enters the formulae as a ratio.

System (19) and (20), along with temperature dynamics (5)–(7) in which emissions in each region are given by the optimal emissions (12), constitute the Hamiltonian system which determines optimal paths for the temperature anomalies ($T_1(t)$, $T_2(t)$), the associated costate variables or shadow costs ($\Lambda_{T_1}(t)$, $\Lambda_{T_2}(t)$), the optimal fossil fuel use (or emission) path in each region $E(x, t)$, and the corresponding steady states.

3.1. Bias from ignoring heat transport

The results of the welfare optimization problem can be used to explore the impact of heat transport and PA on climate policy. In particular we are interested in calculating the error made if the planner mistakenly ignores heat transfer Tr in computing optimal carbon taxes. To calculate this error, we compute the solution by the planner who acts as if $Tr = 0$, but heat transport is present in the actual climate. The planner mistakenly replaces (19) and (20) with

$$\frac{d\widehat{\Lambda}_{T_1}}{dt} = (\rho + B)\widehat{\Lambda}_{T_1} + d_1 \quad (25)$$

$$\frac{d\widehat{\Lambda}_{T_2}}{dt} = (\rho + B)\widehat{\Lambda}_{T_2} + d_2, \quad (26)$$

with the incorrect steady-state externality tax defined by

$$\hat{\tau} = -\lambda(\widehat{\Lambda}_{T_1} + \widehat{\Lambda}_{T_2}) \quad (27)$$

$$\widehat{\Lambda}_{T_1} = \frac{-d_1}{\rho + B}, \quad \widehat{\Lambda}_{T_2} = \frac{-d_2}{\rho + B}. \quad (28)$$

The planner's incorrect tax rate may be compared with the correct steady-state tax rate given in (20). From the definition of the steady states for the costate variables (21) and (22), it is convenient to write the correct tax rate $\tau(\gamma_1, \gamma_2)$ as a function of heat and moisture transport parameters (γ_1, γ_2), or

$$\begin{aligned} \tau(\gamma_1, \gamma_2) &= -\Lambda((\Lambda_{T_1} + \Lambda_{T_2})) \\ &= \frac{\Lambda[(\rho + B + 2\gamma_1)(d_1 + d_2) + 2\gamma_2 d_2]}{(\rho + B)(\rho + B + 2\gamma_1 + \gamma_2)}. \end{aligned} \quad (29)$$

Since the incorrect tax can be written as $\hat{\tau} = \tau(\gamma_1, 0)$, the optimal tax rate is the same as the planner's optimal tax rate unless $\gamma_2 > 0$. The ratio of the planner's incorrect choice of "optimal" tax rate and the true tax rate is

$$\frac{\hat{\tau}}{\tau(\gamma_1, \gamma_2)} = \frac{\tau(\gamma_1, 0)}{\tau(\gamma_1, \gamma_2)} = \frac{(d_1 + d_2)(\rho + B + 2\gamma_1 + \gamma_2)}{(\rho + B + 2\gamma_1)(d_1 + d_2) + 2\gamma_2 d_2}. \quad (30)$$

It is informative to compute relative error in setting tax rates when γ_2 goes to infinity. Using L'Hospital's rule, we obtain

$$\frac{\tau(\gamma_1, \infty)}{\tau(\gamma_1, 0)} = \frac{2d_2}{d_1 + d_2}. \quad (31)$$

We see from (31) that the correct tax rate can be as much as twice the tax rate with no PA due to heat and moisture transport (i.e. when $\gamma_2 = 0$) when the share of region 2's damages $\frac{d_2}{d_1 + d_2}$, is 1. We sum up our discussion in Proposition 1 below.

Proposition 1. *The planner who mistakenly ignores spatial heat transport taxes carbon too little, i.e. $\frac{\tau(\gamma_1, 0)}{\tau(\gamma_1, \gamma_2)} < 1$ if and only if $(d_1 + d_2)\gamma_2 < 2\gamma_2 d_2$. The planner taxes carbon too much if and only if $(d_1 + d_2)\gamma_2 > 2\gamma_2 d_2$.*

Proof. It follows immediately from (30) that:

$$\frac{\hat{\tau}}{\tau(\gamma_1, \gamma_2)} = \frac{\tau(\gamma_1, 0)}{\tau(\gamma_1, \gamma_2)} \leq 1 \text{ iff } (d_1 + d_2)\gamma_2 \leq 2\gamma_2 d_2.$$

□

Since the damage share from the warming of the high latitudes is $s_2 \equiv \frac{d_2}{d_1 + d_2}$, the direction of bias in carbon taxes in this model from ignoring spatial heat transport is described by a very simple relation between the damage shares and the two basic parameters of heat transport. Furthermore, when γ_2 goes to infinity, it can be easily seen by using L'Hospital's rule in (30) and reversing the ratio that

$$\frac{\tau(\gamma_1, \infty)}{\tau(\gamma_1, 0)} = \frac{2d_2}{d_1 + d_2}. \quad (32)$$

Thus, if the share of region 2's damages is close to 1, $s_2 \approx 1$, and the transport parameter γ_2 is very high, the correct tax rate can be as much as twice the tax rate when PA due to heat and moisture transport is ignored (i.e. when $\gamma_2 = 0$). The

Table 1
Parameter values used in the calibration.^a

$\Lambda = 1.7 \pm 0.4^\circ\text{C}$	Transient climate response to cumulative CO ₂ emissions
$\gamma_1 = \gamma_2 = 0.15$	Heat transport parameters
$H = 4.58 \text{ PW year/K}$	Upper ocean layer heat capacity
$d_1 \in [0.01, 0.1]$	Marginal damage parameter (temperature increase in box 1)
$d_2 \in [0.1, 0.2]$	Marginal damage parameter (temperature increase in box 2)
$L_1 = 3.23 \text{ billion}$	Population in box 1
$L_2 = 3.23 \text{ billion}$	Population in box 2
$\alpha = 0.05$	Production elasticity with respect to energy
$\rho = 0.02$	Utility discount rate

^a For a detailed discussion of the parameter selection see [Appendix D](#).

role of $\gamma_2 > 0$ in the above conclusions is crucial. As [Langen and Alexeev \(2007\)](#) and [Alexeev and Jackson \(2013a\)](#) stress, $\gamma_2 > 0$ captures aspects of moisture transport in addition to aspects of heat transport. [Proposition 1](#) shows how neglecting heat and moisture transport in climate economics can lead to bias in the externality tax. Furthermore, [Proposition 1](#) reveals what parameter values determine the direction and the amount of the bias. We believe this is a valuable insight for climate economics.¹⁴

3.1.1. A numerical simulation

In order to obtain more insights into the results derived above, we proceed with a simple numerical simulation of the Hamiltonian system associated with (10). To calibrate the climate part of the model we adopt benchmark estimates from the literature following, in particular, [Langen and Alexeev \(2007\)](#). Also, as mentioned in [Section 3](#), we follow [Golosov et al. \(2014\)](#) in assuming exponential damages. Important parameters of our model are the marginal damage parameters $d_1 = d_{11} + d_{21}$ and $d_2 = d_{12} + d_{22}$. Parameter d_1 reflects damages in both boxes from an increase in temperature in box 1, while d_2 reflects damages in both boxes from an increase in temperature in box 2. Thus, the parameter d_2 embodies damages related to PA in boxes 1 and 2. As discussed in the introduction, damages due to PA-induced temperature increases include increases in damages due to extreme weather events, sea level rise, permafrost feedbacks and political conflicts. These damages are realized in both boxes, since box 2 includes latitudes greater than 30°N. Although the issues of climate change related damages has been extensively discussed, to our knowledge there are no rigorous estimates of parameters d_1 and d_2 in relation to *relative* changes in the corresponding regional temperatures. In [Appendix D](#) we provide a detailed discussion of the calibration parameters which suggests that d_2 could be high relative to the case where PA is ignored and potentially high relative to d_1 .¹⁵ The parameters used in our numerical simulation are summarized in [Table 1](#).

The simulation proceeds as follows. We compute steady states $\mathbf{z} = (T_1, T_2, \Lambda_{T_1}, \Lambda_{T_2})$ from the Hamiltonian system which is obtained by using the climate dynamics (5) and (6) with $E(x, t)$ replaced by (12); the costate dynamics given by (19) and (20); values for d_1 and d_2 in the range of [Table 1](#); and assuming infinite fossil fuel reserves ($\Lambda_{R_0}(t) = 0$) and equal welfare weights. In all runs there is a unique steady state which has the saddle point property with two positive and two negative eigenvalues. For the choice $(d_1, d_2) = (0.05, 0.2)$, the steady state is $\mathbf{z} = (1.578, 2.763, -2.871, -3.942)$, with eigenvalues $\mathbf{e} = (0.140, -0.120, 0.042, -0.022)$. To obtain insights into the optimal paths for the state and the costate variables, we solve the linear approximation of the Hamiltonian system around the steady state. Setting the constants associated with positive eigenvalues equal to zero and using initial and steady-state values for the state variable (temperature anomalies), we compute the remaining constants and the initial values for the costates. We obtain the paths for temperature anomalies and the corresponding costate variables. The paths for the optimal temperature anomalies are shown in [Fig. 2](#), along with the path for the optimal global anomaly resulting under the same parameterization but assuming that heat and moisture transport and PA do not take place. The PA effect under the optimal policy is clear.

Since in our parameterization $d_1 < d_2$ and $s_2 \equiv \frac{d_2}{d_1 + d_2} > 1/2$, we expect that, according to [Proposition 1](#), the optimal externality tax at the steady state will exceed the corresponding “wrong” tax which is calculated by ignoring PA. To put it differently, ignoring PA causes undertaxing. To determine this bias we compute the path for the optimal tax (14) obtained by using the costate paths from the solution of the linearized Hamiltonian system, and we compare it to the “wrong” steady-state externality tax (27). To obtain a ballpark estimate of these carbon taxes in $\$/\text{CO}_2$, we consider logarithmic utility in

¹⁴ A more elaborate model that includes both heat and moisture transport is that of [Fanning and Weaver \(1996\)](#). [Langen and Alexeev \(2007\)](#) and [Alexeev and Jackson \(2013a\)](#) models can be usefully viewed as abstractions that capture aspects of the more complicated [Fanning and Weaver \(1996\)](#) model which, in turn, is a drastic simplification of the more realistic [Weaver et al. \(2001\)](#) model. Using the more realistic models could be useful for serious numerical analysis of coupled climate-economy models, but it is beyond the scope of the present paper. We believe, however, that the analytical clarity in showing how the bias depends upon marginal damages for each of the two regions of latitude belts as well as the two basic parameters of heat and moisture transport counterbalances the cost of abstracting away from more realistic features of damages and heat and moisture transport dynamics.

¹⁵ Furthermore, results presented by [Ceronisky et al. \(2011\)](#) suggest that heat transport from the lower box to the upper box magnified by PA should incrementally increase the probability of events like the Greenland ice sheet melt, which in turn increase the damages due to increased flooding in places like Bangladesh and other poor areas in the lower box where many poor people live and the land is cheaper due to flooding risk. This argument suggests that the parameter d_{12} is likely to be relatively large.

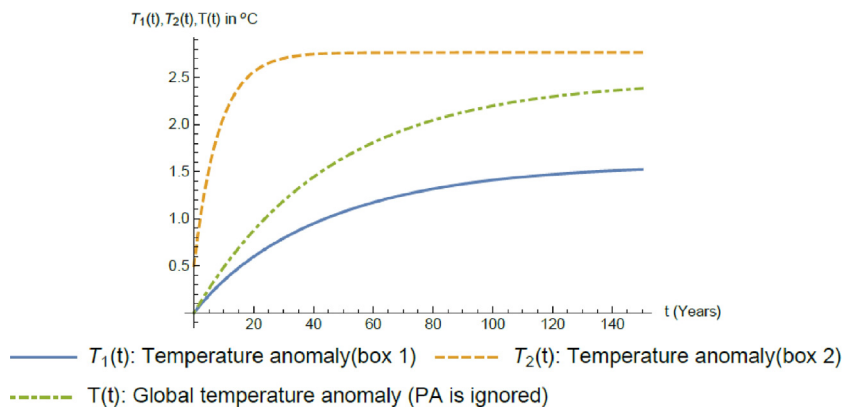


Fig. 2. Temperature anomalies.

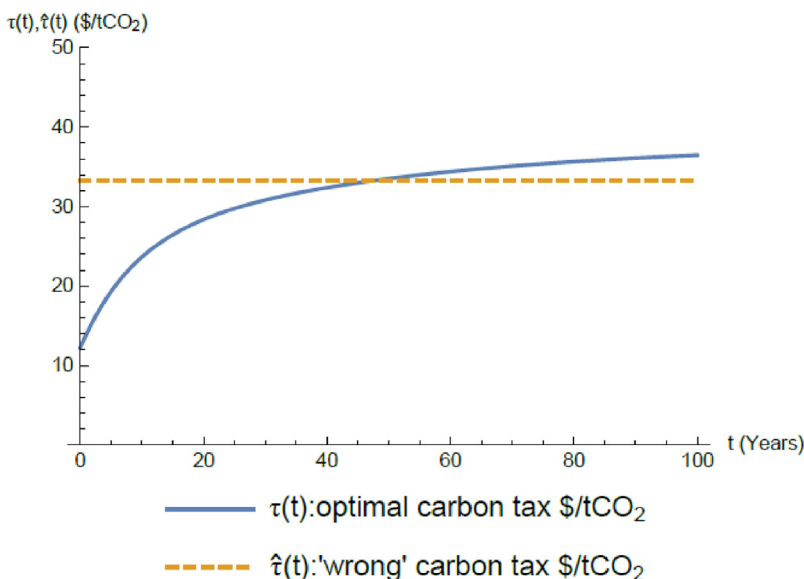


Fig. 3. Optimal vs. "wrong" carbon taxes.

consumption and divide the taxes by marginal utility. This is equivalent to multiplying the taxes by consumption.¹⁶ Then, since our TCRE parameter, Λ , is expressed in $^{\circ}\text{C}/\text{GtCarbon}$, we divide the result by 3.67 to transform it in terms of CO_2 since 1 tonne of carbon = 3.67 tonnes of CO_2 . The carbon taxes are shown in Fig. 3. At the steady state the optimal tax exceeds the "wrong" tax by 12.3%.

The basic result that emerges from our simulations is that the bias in the carbon tax from ignoring PA ranges from of 6% to 20%. The bias increases with the deviation between d_1 and d_2 . It should be noted, however, that since our model is highly stylized, the results of our simulations can be regarded only as ballpark estimates, which crucially depend on the marginal damage values.¹⁷ These estimates, which confirm our analytical results, provide insights about the type of results that we expect from highly complex models, which would provide more accurate numerical estimates but not analytical results.¹⁸

¹⁶ We use global consumption for 2015 in current US\$ from the database World Development Indicators.

¹⁷ TFP growth is not included in our model. In the logarithmic utility case, a rapid increase in $C(t) = 1/U'(C(t))$ due to TFP increasing will shift the tax schedules upwards.

¹⁸ Cai et al. (2017), in the spatial extension of the stochastic DSICE, calculate the same tax bias to be between 10% and 20%.

4. The welfare cost of ignoring heat and moisture transport

While the computation of qualitative effects of spatial transport on optimal emissions tax rates analyzed above is useful, it does not tell us much about the economic importance of taking spatial heat and moisture into account. For this, we need to compute the impact on economic welfare measures. We turn to this task now.

Suppose a planner mistakenly believes that heat and moisture transport is not present, i.e. $(\gamma_1, \gamma_2) = (0, 0)$, but the true dynamics are $\gamma_1 > 0, \gamma_2 > 0$. How big is the error in welfare units and how big is the error in energy use and emissions taxes? We formulate a conceptual framework and study these questions here.

Consider the social welfare optimization problem

$$V[(\gamma_1, \gamma_2) | (\gamma_1, \gamma_2)] \equiv \max \int_{t=0}^{\infty} e^{-(\rho-\eta)t} \left[\sum_{x=1}^{x=2} v(x)L(x, t) \ln[y(x, t)E(x, t)^\alpha e^{-\phi(x)(T)}] \right] dt \tag{33}$$

subject to (5) – (7) and (13),

where we denote by $V[(\gamma_1, \gamma_2) | (\gamma_1, \gamma_2)]$ the optimal value when the planner believes the transport parameters are (γ_1, γ_2) and the true transport parameters are (γ_1, γ_2) .¹⁹ We denote the value when the planner believes the transport parameters $(a_1, a_2) \neq (\gamma_1, \gamma_2)$, but the true transport parameters are (γ_1, γ_2) by $V[(a_1, a_2) | (\gamma_1, \gamma_2)]$. Then, by construction, we have

$$V[(a_1, a_2) | (\gamma_1, \gamma_2)] \leq V[(\gamma_1, \gamma_2) | (\gamma_1, \gamma_2)], \tag{34}$$

for all $(a_1, a_2) \geq (0, 0)$. Hence the welfare cost of the error made by a planner who believes (a_1, a_2) when the true parameters are (γ_1, γ_2) is:

$$\psi = V[(\gamma_1, \gamma_2) | (\gamma_1, \gamma_2)] - V[(a_1, a_2) | (\gamma_1, \gamma_2)] \geq 0. \tag{35}$$

We use similar notation for total emissions at date t , $E[(a_1, a_2) | (\gamma_1, \gamma_2)]$ and the temperature anomalies $T_i[(a_1, a_2) | (\gamma_1, \gamma_2)]$, $i = 1, 2$ for the planner who believes the transport parameters are (a_1, a_2) but the true parameters are (γ_1, γ_2) . The computational procedure for determining the welfare cost can borrow a lot of material from Section 3, once we recognize that when (γ_1, γ_2) is replaced by (a_1, a_2) in (19) and (20), the beliefs of the planner about the parameters of the temperature dynamics determine the costate variables for the two temperature anomalies, as²⁰

$$\dot{\Lambda}_{T_1} = [\rho - \eta + (B + a_1 + a_2)]\Lambda_{T_1} - [(a_1 + a_2)]\Lambda_{T_2} + d_1 \tag{36}$$

$$\dot{\Lambda}_{T_2} = -a_1 \Lambda_{T_1} + [\rho - \eta + (B + a_1)]\Lambda_{T_2} + d_2. \tag{37}$$

The steady-state solutions for the costate variables are given by (21) and (22) with (γ_1, γ_2) replaced by (a_1, a_2) . Furthermore, the planner's beliefs determine the steady-state externality tax as:

$$\tau(a_1, a_2) = -\Lambda(\Lambda_{T_1} + \Lambda_{T_2}) = \frac{\Lambda[(\rho - \eta + B + 2a_1)(d_1 + d_2) + 2a_2d_2]}{(\rho - \eta + B)(\rho - \eta + B + 2a_1 + a_2)}, \tag{38}$$

which in turn determines emissions according to

$$E(x, t, (a_1, a_2)) = \frac{\alpha v(x)L_0(x)}{\tau(a_1, a_2) + \Lambda_{R_0}(a_1, a_2)e^{(\rho-\eta)t}}. \tag{39}$$

Note that for the infinite reserve case, $\Lambda_{R_0}(a_1, a_2) = 0$. The true transport parameters and emissions chosen under wrong beliefs now determine the actual paths of the temperature anomalies,

$$\dot{T}_1 = [(-B - \gamma_1 - \gamma_2)T_1 + \gamma_1 T_2 + \Lambda E(t, (a_1, a_2))], \quad T_1(0) = 0 \tag{40}$$

$$\dot{T}_2 = [(\gamma_1 + \gamma_2)T_1 + (-B - \gamma_1)T_2 + \Lambda E(t, (a_1, a_2))], \quad T_2(0) = 0. \tag{41}$$

This setup allows us to obtain the steady-state welfare cost when the planner uses wrong beliefs to determine the optimal carbon tax. The bounds of the welfare cost are provided in the following proposition.

Proposition 2. *The welfare cost ψ of wrong beliefs about transport parameters is bounded below by $[1 - \ln(2)] \sum_{x=1}^{x=2} \alpha v(x)L_0(x)$, and tends to infinity when the share of marginal damages, s_2 , is zero and $\gamma_2 \rightarrow \infty$.*

For the proof, see Appendix 3.

¹⁹ Here, as in Section 2, $T(t) = T_b + T(t)$ and we have assumed that population grows at the same rate η in each region, so that $L(x, t) = L_0(x)e^{\eta t}$.

²⁰ Note that we have set $H = 1$.

The main message from [Proposition 2](#) is that it is very important to avoid the mistaken belief that γ_2 is small when the damage share of the high latitudes is small and the true value of γ_2 is large. To obtain an indication of welfare cost in terms of consumption, we consider the amount ΔC that welfare under correct beliefs $V[(\gamma_1, \gamma_2) | (\gamma_1, \gamma_2)]$ should be reduced to become equal to welfare under wrong beliefs $V[(a_1, a_2) | (\gamma_1, \gamma_2)]$, or

$$V[(\gamma_1, \gamma_2) | (\gamma_1, \gamma_2); \Delta C] = V[(a_1, a_2) | (\gamma_1, \gamma_2)]. \quad (42)$$

The term ΔC , acting as an equivalent variation, is a measure of how much it is worth in consumption units to use the correct heat transport parameters and therefore to account for PA.

To compute such a measure, we use the optimized steady-state welfare derived in [Appendix C Eq. \(C.12\)](#), as

$$W[(a_1, a_2) | (\gamma_1, \gamma_2)] \equiv \max \left\{ \sum_{x=1}^{x=2} \alpha \nu(x) L_0(x) \ln E((a_1, a_2), x) - [E((a_1, a_2), 1) + E((a_1, a_2), 2)] h(\gamma_1, \gamma_2) \right\},$$

to define

$$W(\gamma_1, \gamma_2 | \gamma_1, \gamma_2; \Delta C) = \sum_{x=1}^{x=2} \nu(x) L_0(x) \ln [E(\gamma_1, \gamma_2, x)^\alpha \exp(-E(\gamma_1, \gamma_2, x) h(\gamma_1, \gamma_2)) - \Delta C]$$

$$W(\alpha_1, \alpha_2 | \gamma_1, \gamma_2) = \sum_{x=1}^{x=2} \nu(x) L_0(x) \ln [E(\alpha_1, \alpha_2, x)^\alpha \exp(-E(\alpha_1, \alpha_2, x) h(\gamma_1, \gamma_2))],$$

where $E(\alpha_1, \alpha_2, x)$, $E(\gamma_1, \gamma_2, x)$ are the optimal emissions. Then the equivalent variation ΔC solves

$$W(\gamma_1, \gamma_2 | \gamma_1, \gamma_2; \Delta C) - W(\alpha_1, \alpha_2 | \gamma_1, \gamma_2) = 0. \quad (43)$$

Considering $C^* = E(\gamma_1, \gamma_2, x)^\alpha \exp(-E(\gamma_1, \gamma_2, x) h(\gamma_1, \gamma_2))$, at the steady-state optimal $E(\gamma_1, \gamma_2, x)^\alpha$, as a measure of effective consumption in each region when heat and moisture transfer is taken into account and using the parameterization of [Section 3.1.1](#), we computed the ratio $\Delta C/C^*$ for $(\gamma_1, \gamma_2) = (0.15, 0.15)$ and $(\alpha_1, \alpha_2) \in [0, 0.15] \times [0, 0.15]$.²¹ This ratio can be interpreted as a measure of welfare loss in consumption terms from ignoring PA. For our parameterization this loss ranges from 2% to 0.15%. The highest loss emerges when $\gamma_2 = 0.15$ and $\alpha_2 = 0$. Note, however, this measure is obtained under specific restrictions of our simplified model and in this respect is a ballpark estimate. On the other hand, the numerical exercise confirms our theoretical prediction, and we think that it indicates the result that would be obtained from a more complex model.

5. Conclusions and areas for further research

Polar amplification is an established scientific fact which has been associated with the surface albedo feedback and, through recent research, to heat and moisture transport from the Equator to the Poles. In the present paper we unify a two-box (or two-region) climate model, which allows for heat and moisture transport from the southern region to the northern region, with an economic model of welfare optimization. In the economic model, a regulator chooses fossil fuel use which is equivalent to GHG emissions. Emissions induce the temperature anomaly, relative to baseline temperature in the two regions, along with damages from temperature increase over the baseline.

Our main contribution is to show that, by ignoring spatial heat and moisture transport and the resulting PA, the regulator may introduce a bias on the tax on GHG emissions. The direction of bias depends on the relations between marginal damages from a temperature increase in each region. If, as expected, marginal damages due to a temperature increase in the North exceed marginal damages from a corresponding increase in the South, due to PA and Arctic amplification effects that affect both regions, then ignoring spatial heat and moisture transport could underestimate the optimal tax. A ballpark estimate from our highly stylized model suggests that this bias could reach 20% depending on marginal damages discrepancies. We also determine the welfare cost when a regulator mistakenly ignores spatial heat and moisture transport. Numerical simulations suggest that a ballpark estimate, obtained by using an equivalent variation type of measure of welfare cost in consumption terms, is in the range of 0.15–2% of steady-state effective consumption.

Regarding the numerical estimates, our model – like many stylized abstract models – is meant only to be suggestive of what a more realistic exercise might find. Complex models, like most of the IAMs, are difficult to comprehend, especially regarding the emergence of the numerical results ([van der Ploeg and Rezai, 2016](#)). On the other hand, relatively simple models like the one presented here have the virtue of simplicity and transparency, while the theoretical predictions seem to be confirmed by the numerical exercises.

Our framework can be used to calculate the discount rate for discounting cost and benefit flows in cost-benefit analysis. Preliminary results indicate that heat and moisture transport and the PA effect, through the growth of emissions in one

²¹ For $(\alpha_1, \alpha_2) = (0.15, 0.15)$, $\Delta C = 0$.

region, induce an adjustment to the standard Ramsey rule used to determine the discount rate for cost-benefit analysis in the other region. This result could be important in evaluating investment projects related to climate change.

In order to produce analytic results, our economic model is simple and does not allow for capital accumulation. An interesting area for further research would be to explore how the two-region model with PA can be unified with a Ramsey-type optimal growth model. Some preliminary numerical simulations indicate that the steady states of the economic and the climate systems obtained with and without spatial heat and moisture transport differ from each other. These results suggest that ignoring spatial phenomena and PA in climate change may result in suboptimal policies when more realistic growth models are considered.

In the context of the present results, it would be interesting to study the impact of heat transport and PA on the potential spatial differentiation of carbon taxes between rich and poor regions when compensatory transfers among regions are costly or not possible. Another interesting extension, which is gaining popularity in climate change models (e.g., Cai et al., 2015a; Jensen and Traeger, 2014), would be to use Epstein–Zin preferences, which can distinguish between preferences for risk and time, in the two-box model with local differentiation of these preferences.

Additional further research – apart from introducing factors like human capital, R&D, uncertainty, or nonlinearities induced by SAF and tipping points – could study pollution externalities from fossil fuel emissions. Their effects can be modeled by introducing an extra state variable for each box together with transport across the two boxes. Some of these externalities may be as important as the climate change externalities.²²

Appendix A. The linear relationship between ΔT and $CE(t)$

Following MacDougal and Friedlingstein (2015), two well-established relationships indicate that: (i) the change in temperature ΔT is proportional to the difference between the radiative force F and the planetary heat uptake ΔQ , or

$$F = \lambda \Delta T + \Delta Q, \tag{A.1}$$

where λ is the climate feedback parameter, and (ii) transient climate response to cumulative CO₂ emissions (TCRE) is defined (Matthews et al., 2009) as:

$$\Lambda = \frac{\Delta T(t)}{CE(t)}, \tag{A.2}$$

where $CE(t)$ are cumulative carbon emissions up to time t . Approximating the radiative forcing from CO₂ using the classical logarithmic relationship $F = R \ln(1 + \frac{\alpha CE(t)}{C_0})$, where R is the radiative forcing for an e -fold increase in atmospheric CO₂ concentration, α is the airborne fraction of emitted carbon, C_0 is the original quantity of carbon in the atmosphere, and using the appropriate definition for ΔQ , MacDougal and Friedlingstein (2015) derive the change in temperature as a function of cumulative emissions by²³

$$\Delta T(t) = \frac{R}{\lambda} \ln\left(1 + \frac{\alpha CE(t)}{C_0}\right) \left(\frac{1}{1 + 1/\sqrt{\phi \lambda^2 t}}\right). \tag{A.3}$$

MacDougal and Friedlingstein (2015) show that (A.3) leads to an approximately constant value, Λ , for the TCRE which suggests a linear relationship between a change of global average temperature and cumulative emissions. This linear relationship (see also Matthews et al., 2009; 2012) has also been recognized by the IPCC (2013).

To obtain a clearer picture of this near-linear relationship, we computed $\Delta T(t)$ from (A.3), using MacDougal and Friedlingstein's (2015, Table 1) parameterization. We calculated cumulative emissions from annual data in billion tonnes of carbon per year (GtC/yr) for the period 1959–2015, on global carbon emissions from fossil fuel combustion and cement production, plus emissions from land-use change.²⁴ The relationship between the computed $\Delta T(t)$ vs. $CE(t)$ is shown in Fig. A1.

In the graph the dotted line is the computed points ($CE(t)$, $\Delta T(t)$) and the solid line is the fitted linear relationship. It is clear that the near-linear relationship is supported.²⁵ An ideal approach would be to do a robustness analysis where the true relation is surrounded by an envelope of approximations and policy optimization is done against the worst case model in this cloud of approximate models.²⁶ This is, however, beyond the scope of the current paper.

²² For example, Parry et al. (2014) estimate co-benefits from the control of such pollutants for 20 major polluting countries. They show that co-benefits vary widely across the 20 countries but are substantial for all of them.

²³ Note that in comparison to MacDougal and Friedlingstein (2015, Eq. (9), p. 4220), in (A.3) we have replaced their simplifying assumption that $CE(t) = rt$ with a general path of cumulative emissions $CE(t)$.

²⁴ The source is Global Carbon Budget, <http://www.globalcarbonproject.org/carbonbudget/16/data.htm>.

²⁵ MacDougal and Friedlingstein (2015) provide an excellent discussion of the origins of this approximate linearity, the range of scales where it approximately holds, and where it is likely to fail.

²⁶ For an exposition of robust control methods, see for example Hansen and Sargent (2008). For application of robust control to climate policies, see for example Athanassoglou and Xepapadeas (2012).

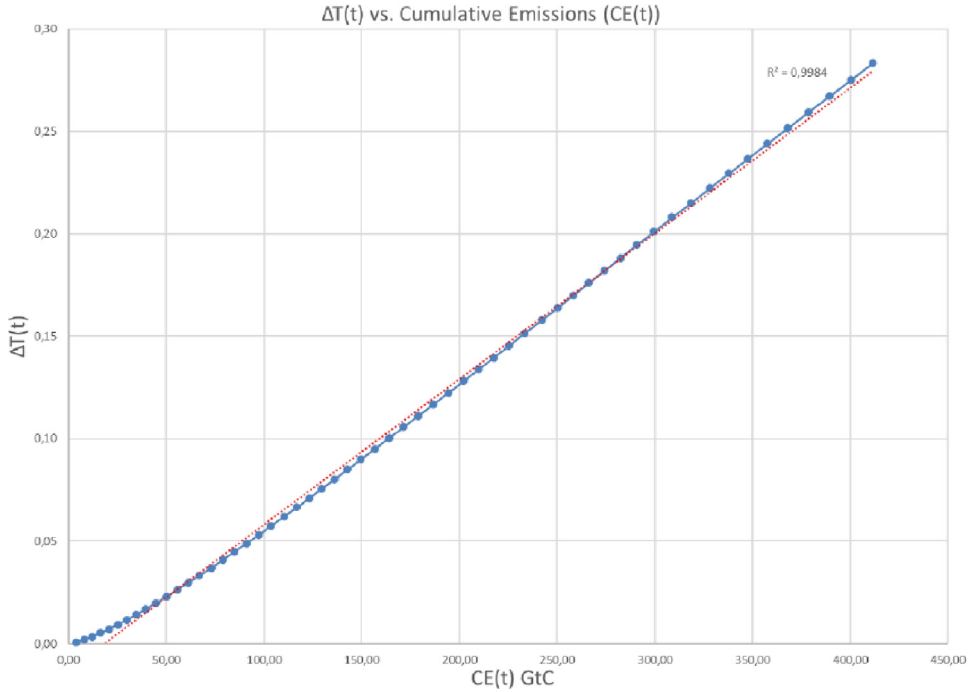


Fig. A1. Temperature vs. cumulative emissions.

In the context of the near proportional relationship between $CE(t)$ and $\Delta T(t)$, the anthropogenic impact on the global temperature increase can be approximated in continuous time by

$$T(t) - T(0) = \Lambda \int_{s=0}^t E(s) ds, \quad (\text{A.4})$$

where $CE(t) = \int_{s=0}^t E(s) ds$ denotes cumulative global carbon emissions up to time t and Λ is the TCRE. Taking the time derivative of (A.4), we obtain

$$\dot{T}(t) = \Lambda E(t). \quad (\text{A.5})$$

We consider this continuous time approximation as a useful short cut, which is supported by climate science, so that simple optimal control theory can be used to provide insights and suggest the direction of biases when PA is ignored. Thus our abstraction using $\dot{T}(t) = \Lambda E(t)$ allows the use of simple mathematical modeling in a two-box model. Note that the two-box model is also an abstraction which is, however, very helpful in providing insights about the mechanisms driving PA.

Appendix B. The impact of the sea-ice albedo feedback

While the model (1) and (2) strictly represents a form of PA based on changes in the meridional heat transport, latent heat transport (Langen and Alexeev, 2007, p. 309), the SAF is regarded as an important PA mechanism. This mechanism in which the albedo is assumed to depend on temperature is not captured by model (1) and (2). However, this model can be easily modified to allow for a simple SAF mechanism in the following way.

In model (1) and (2) replace S_1 by $\alpha_1 S_1$ and S_2 by $S_2[1 + \alpha_2(T_{2b} + T_2)]$, $(\alpha_1, \alpha_2) > (0, 0)$, where $\alpha_2(T_{2b} + T_2)$ is the co-albedo SAF feedback term which increases as temperature increases because more of the solar S_2 gets absorbed and is not reflected into space as the sea ice continues to shrink. It is reasonable to assume that $\alpha_1 S_1$ is approximately constant, thus after substituting the new S_1 and S_2 into (1) and (2) we obtain:

$$\dot{T}_1 = \frac{1}{H} [(-B - \gamma_1 - \gamma_2)T_1 + \gamma_1 T_2 + \Lambda E(t)] \quad (\text{B.1})$$

$$\dot{T}_2 = \frac{1}{H} [(\gamma_1 + \gamma_2)T_1 + (-B - \gamma_1 + \alpha_2 S_2)T_2 + \Lambda E(t)]. \quad (\text{B.2})$$

In model (B.1) and (B.2), $\alpha_2 = 0$ implies that the SAF mechanism is not included, while $\gamma_2 = 0$ implies that the effect of an increased moisture supply and thus greater latent heat transport (Langen and Alexeev, 2007, p. 309) is not included.

Assume again that $E(t) = E$ constant and let (T_1^*, T_2^*) be the steady state and J the Jacobian matrix of (B.1) and (B.2). If $\text{tr}(J) = -2B - 2\gamma_1 - \gamma_2 + \alpha_2 S_2 < 0$, and $\det(J) = B(+2\gamma_1 + \gamma_2) - \alpha_2(B + \gamma_1 + \gamma_2)S_2 > 0$, this steady state is stable. Denote by $\mathcal{D}(\gamma_2, \alpha_2)$ the difference, $T_2^* - T_1^*$, between the two steady states, then

$$\mathcal{D}(\gamma_2, \alpha_2) = \frac{2E\Lambda\gamma_2 + E\Lambda\alpha_2S_2}{B(B + 2\gamma_1 + \gamma_2) - \alpha_2(B + \gamma_1 + \gamma_2)S_2} \tag{B.3}$$

$$\mathcal{D}(\gamma_2, 0) = \frac{2E\Lambda\gamma_2}{B(B + 2\gamma_1 + \gamma_2)} \tag{B.4}$$

$$\mathcal{D}(0, \alpha_2) = \frac{E\Lambda\alpha_2S_2}{B(B + 2\gamma_1) - \alpha_2(B + \gamma_1)S_2} \tag{B.5}$$

$$\mathcal{D}(0, 0) = 0. \tag{B.6}$$

From the stability conditions it is clear that $\mathcal{D}(\gamma_2, \alpha_2) > \mathcal{D}(\gamma_2, 0)$. Thus when the SAF effect is added we can see that this new steady-state temperature vector has higher temperatures than the steady state without the SAF effect for each fixed level of constant $E(t)$. Furthermore it is clear that symmetry in the steady-state temperature vector breaks when either of the two mechanisms is present. In the paper we set, in order to keep the model simpler and to reduce the numbers of parameters required for simulations, $\alpha_2 = 0$ and concentrate on the effects of the meridional heat transport and other heat transport. The results above and the fact that the SAF effect increases only the coefficient of T_2 in the temperature-dynamics Eq. (6) suggests that the qualitative nature of our results regarding optimal taxes and welfare losses obtained with $\alpha_2 = 0$ will not change when $\alpha_2 > 0$.²⁷ Our conjecture is that, with the SAF effect added, the box 2 temperature will be higher and thus any damage flow towards box 1 caused by higher temperature in box 2 will be increased.

Appendix C. Proof of Proposition 2

In computing the welfare effects, it is convenient to separate out in (33) the term

$$\int_{t=0}^{\infty} e^{-(\rho-\eta)t} \left[\sum_{x=1}^{x=2} v(x)L_0(x)\ln[y_0(x, t) - \phi(x)T_b(x)] \right] dt, \tag{C.1}$$

which does not vary with emissions, and compute the component of welfare which does vary with emissions. Hence we focus on the variable component of welfare in Eq. (C.2) below. We denote this component, when beliefs are correct, by

$$W[(\gamma_1, \gamma_2) | (\gamma_1, \gamma_2)] \equiv \max \int_{t=0}^{\infty} e^{-(\rho-\eta)t} \left[\sum_{x=1}^{x=2} v(x)L_0(x)\ln[E(x, t)^\alpha e^{-\phi(x)T_x(t)}] \right] dt, \tag{C.2}$$

with analogous notation for the variable component of welfare, $W[(a_1, a_2) | (\gamma_1, \gamma_2)]$, when beliefs about the parameters of the temperature anomaly dynamics are (a_1, a_2) but the true parameters are (γ_1, γ_2) . It is very tedious to compute $W[(a_1, a_2) | (\gamma_1, \gamma_2)]$ for the case of finite known reserves, R_0 , so we proceed as follows, noting that from the FONC, optimal emissions when the tax is $\tau(a_1, a_2)$ are given by (39). In the variable welfare component (C.2), substitute optimal emissions (39) and steady-state temperature anomalies

$$T_1 = \frac{\alpha\Lambda[v(1)L_0(1) + v(2)L_0(2)](B + 2\gamma_2)}{B(B + 2\gamma_1 + \gamma_2)[\tau(a_1, a_2) + \Lambda_{R_0}(0)e^{(\rho-\eta)t}]} \tag{C.3}$$

$$T_2 = \frac{\alpha\Lambda[v(1)L_0(1) + v(2)L_0(2)][B + 2(\gamma_1 + \gamma_2)]}{B(B + 2\gamma_1 + \gamma_2)[\tau(a_1, a_2) + \Lambda_{R_0}(0)e^{(\rho-\eta)t}]}, \tag{C.4}$$

which are obtained from (40) and (41) after setting $\dot{T}_1 = \dot{T}_2 = 0$ and solving the linear system for (T_1, T_2) . Next we gather all terms in $W[(a_1, a_2) | (\gamma_1, \gamma_2)]$ that are common to $\tau(a_1, a_2) + \Lambda_{R_0}(a_1, a_2)e^{(\rho-\eta)t}$, and separate out terms in $W[(a_1, a_2) | (\gamma_1, \gamma_2)]$ that are not. Define the following quantities:

$$w_1 = \sum_{x=1}^{x=2} v(x)L_0(x)[\alpha\ln(\alpha v(x)L_0(x))] \tag{C.5}$$

²⁷ A possible complication with the SAF effect in more general models is that it may introduce nonlinearities and the possibility of multiple steady states. Calibrating nonlinear terms using, for example, information from Wagner and Eisenman (2015) is beyond the scope of the current article and represents an area for further research.

$$w_2 = \sum_{x=1}^{x=2} v(x)L_0(x) \tag{C.6}$$

$$w_3 = \frac{\Lambda \left(\sum_{x=1}^{x=2} \alpha v(x)L_0(x) \right)}{D_T} \times [v(1)\phi(1)(B + 2\gamma_1) + v(2)\phi(2)(B + 2\gamma_1 + 2\gamma_2)] \tag{C.7}$$

$$D_T = (B + \gamma_1)(B + \gamma_1 + \gamma_2) - \gamma_1(\gamma_1 + \gamma_2). \tag{C.8}$$

Using these quantities we obtain

$$W[(a_1, a_2) | (\gamma_1, \gamma_2)] = \tag{C.9}$$

$$\int_{t=0}^{\infty} e^{-(\rho-\eta)t} \left[w_1 - w_2 \ln(\zeta(a_1, a_2)) - \frac{w_3}{\zeta(a_1, a_2)} \right] dt \tag{C.10}$$

$$\zeta(a_1, a_2) = \tau(a_1, a_2) + \Lambda_{R_0}(a_1, a_2)e^{(\rho-\eta)t},$$

where $\Lambda_{R_0}(a_1, a_2)$ solves the equation

$$\int_{t=0}^{\infty} \left[\sum_{x=1}^{x=2} \frac{\alpha v(x)L_0(x)}{\zeta(a_1, a_2)} \right] dt = R_0. \tag{C.11}$$

We can obtain some insight by computing $W[(a_1, a_2)|(\gamma_1, \gamma_2)]$ for the case of infinite known reserves because in this case $\Lambda_{R_0}(a_1, a_2) = 0$ and we can obtain steady states and compute $W[(a_1, a_2)|(\gamma_1, \gamma_2)]$ for these steady states. However, we know that unless $\hat{\rho} \equiv \rho - \eta = 0$, optimal steady states do not typically solve a maximization problem. Hence we restrict ourselves to the study of steady states for the case $\hat{\rho} \equiv \rho - \eta = 0$ and adjust the values of the weights $w_i, i = 1, 2, 3$ accordingly.

When $\hat{\rho} \equiv \rho - \eta = 0$, an optimal steady state solves the problem

$$W[(a_1, a_2) | (\gamma_1, \gamma_2)] \equiv \max \left\{ \sum_{x=1}^{x=2} \alpha v(x)L_0(x) \ln E((a_1, a_2), x) - [E((a_1, a_2), 1) + E((a_1, a_2), 2)]h(\gamma_1, \gamma_2) \right\}, \tag{C.12}$$

where

$$d(x) \equiv v(x)L_0(x)\phi(x), \quad x = 1, 2 \tag{C.13}$$

$$h(\gamma_1, \gamma_2) = \tag{C.14}$$

$$\frac{\Lambda}{D_T(\gamma_1, \gamma_2)} [d(1)(B + 2\gamma_1) + d(2)(B + 2\gamma_1 + 2\gamma_2)] \tag{C.15}$$

$$D_T(\gamma_1, \gamma_2) \equiv (B + \gamma_1)(B + \gamma_1 + \gamma_2) - \gamma_1(\gamma_1 + \gamma_2),$$

and $\{E((a_1, a_2), x), x = 1, 2\}$ solves the problem

$$\max_{E(1), E(2)} \left\{ \sum_{x=1}^{x=2} \alpha v(x)L_0(x) \ln E(x) - [E(1) + E(2)]h(a_1, a_2) \right\}. \tag{C.16}$$

We may now compute

$$W[(\gamma_1, \gamma_2) | (\gamma_1, \gamma_2)] - W[(a_1, a_2) | (\gamma_1, \gamma_2)] = \left[[z - \ln(z + 1)] \left[\sum_{x=1}^{x=2} \alpha v(x)L_0(x) \right] \right], \tag{C.17}$$

$$z \equiv \frac{h(\gamma_1, \gamma_2)}{h(a_1, a_2)}. \tag{C.18}$$

Since the function $z - (\ln z + 1)$ is strictly convex and takes a unique minimum at $z = 1$, then,

$$z - (\ln z + 1) > 0, \text{ for all } z \neq 1. \tag{C.19}$$

Using (C.14) we examine the ratio $\frac{h(\gamma_1, \gamma_2)}{h(0, a)}$ to determine how far from 1 it can be. Some tedious algebra yields the formula

$$\frac{h(\gamma_1, \gamma_2)}{h(0, 0)} = \frac{1}{(B + 2\gamma_1 + \gamma_2)} [B + 2\gamma_1 s_1 + 2(\gamma_1 + \gamma_2) s_2] \tag{C.20}$$

$$s_i \equiv \frac{d(i)}{d(1) + d(2)}, i = 1, 2. \tag{C.21}$$

Note that when $\gamma_2 = 0$, we have $\frac{h(\gamma_1, 0)}{h(0, 0)} = 1$. If $\gamma_2 \rightarrow \infty$, then $\frac{h(\gamma_1, \gamma_2)}{h(0, 0)} \rightarrow 2s_2$. Some additional algebra shows that if $s_2 = 0$, then $\gamma_2 \rightarrow \infty$ implies $\frac{h(\gamma_1, \gamma_2)}{h(0, 0)} \rightarrow 0$ and also it is always the case that $\frac{h(\gamma_1, \gamma_2)}{h(0, 0)} \leq 2$. Hence the furthest from 1 for the ratio $\frac{h(\gamma_1, \gamma_2)}{h(0, 0)}$ are the extreme points 0 and 2. If $z \equiv \frac{h(\gamma_1, \gamma_2)}{h(0, 0)}$ in (C.17) and (C.18), we see that the “loss” is infinite when $z \rightarrow 0$. Therefore the bounds on the welfare cost of wrong beliefs about transport parameters can be determined as:

$$\psi = W[(\gamma_1, \gamma_2) | (\gamma_1, \gamma_2)] - W[(a_1, a_2) | (\gamma_1, \gamma_2)] \rightarrow \infty, \text{ when } z \rightarrow 0 \tag{C.22}$$

$$\psi = W[(\gamma_1, \gamma_2) | (\gamma_1, \gamma_2)] - W[(a_1, a_2) | (\gamma_1, \gamma_2)] \rightarrow [1 - \ln(2)] \sum_{x=1}^{x=2} \alpha v(x) L_0(x), \tag{C.23}$$

when $z \rightarrow 2$.

Appendix D. Calibration

In order to obtain more insights into the results obtained above, we proceed with a simple numerical exercise of the Hamiltonian system associated with (10). To calibrate the model we adopt benchmark estimates from the literature. In particular, following [Langen and Alexeev \(2007\)](#), we set $B = 0.1$ PW/K (1 PW is 10^{15} W), $\gamma_1 = \gamma_2 = 0.15$ PW/K. For the heat capacity $H = \pi a_e^2 \rho_d c_w H_d$, we use the condition $\tau_s = H/B$, where, as in [Langen and Alexeev \(2007\)](#), $\tau_s = (5.5 \times 100 \text{ months})/12$ and $B = 0.1$ PW/K, which implies that $H = 4.58$ (PW year)/K. For the value of the cumulative carbon response parameter Λ , we follow [Leduc et al. \(2016\)](#) who provide a global value of $1.7 \pm 0.4^\circ\text{C}$ per TtC, and set $\Lambda = 1.7$. As mentioned in [Section 3](#), we follow [Golosov et al. \(2014\)](#) in assuming exponential damages. Regarding the damage parameter in $\exp(-\phi(x; T))$, we follow [Brock et al. \(2013\)](#) and set the damage parameter of an exponential damage function to 0.01. This value is considered to provide a decent approximation of the quadratic damage function used in [Nordhaus \(2007\)](#) (e.g. a temperature increase of 4°C corresponds to a 5% loss of output). However, we caution that the value of 0.01 was set for a global scale model, not for the scale of a latitude-belt box model.

The marginal damage parameters in our model are $d_1 = d_{11} + d_{21}$ and $d_2 = d_{12} + d_{22}$. Parameter d_1 reflects damages in both boxes from an increase in temperature in box 1, while d_2 reflects damages in both boxes from an increase in temperature in box 2. Thus, the parameter d_2 embodies damages related to PA in boxes 1 and 2.

As discussed in the introduction, damages due to PA-induced temperature increases include increases in damages due to extreme weather events, sea level rise, permafrost feedbacks and political conflicts. These damages are realized in both boxes, since box 2 includes latitudes greater than 30°N . However, to our knowledge there are no rigorous estimates of these parameters in relation to *relative* changes in the corresponding regional temperatures.

Of course, to be clear, there are regional damage estimates in the literature. The output of Nordhaus’s RICE2010,²⁸ for example, provides projections of climate damages per decade for the RICE’s regions, along with projections of atmospheric planetary temperature above preindustrial levels, without, however, regional differentiation of temperatures. According to these estimates, between 2005–2105 total damages as a fraction of gross output are expected to increase from 0.001 to 0.0191 in the USA, from 0.011 to 0.0296 in the EU, from 0.0048 to 0.0389 in India, and from 0.0042 to 0.05 in Africa. The USA and the EU can be regarded as box 2 regions and India and Africa as box 1 regions. Hence, these estimates provide some indications of damage differentiation across boxes.

Our emphasis on differentiation of regional damages due to relative increases in regional temperatures rather than just global increases in temperature is also supported by a considerable literature suggesting that the poorest and most vulnerable groups will disproportionately experience the negative effects of climate change and that such changes are likely to impact significantly on developing world countries, where natural-resource dependency is high. Results from a study of the economic impacts of climate change in which results suggest that in the 21st century climate change is likely to have a limited impact on the economy, and that negative impacts will be substantially greater in poorer, hotter, and lower-lying countries (see also [Mendelsohn, 2009](#); [Thomas and Twyman, 2005](#)). Furthermore, since the climate system transports heat from the lower box (box 1) to the upper box (box 2) and since the upper box contains mostly richer countries with better adaptive capacity, the heat transport from the lower box to the upper box does not incrementally damage the upper box

²⁸ See http://www.econ.yale.edu/~nordhaus/homepage/documents/RICE_042510.xlsm.

much more compared to the non-PA heat transport case. This argument suggests that the parameter d_{21} is likely to be relatively small. These results seem to suggest that marginal damages in box 1 will most likely be higher than in box 2; they do not, however, provide clear insight regarding damages in box 1 and box 2 due to temperature increase in box 1, which is the parameter d_1 .

Regarding d_2 , some insights can be obtained from results regarding damages due to sea level rise (SLR). The IPCC (2013) reports that the rate of SLR since the mid-19th century has been higher than the mean rate during the previous two millennia, and that over the period 1993–2010, global mean SLR was, with high confidence, 2.8 mm/yr. According to the IPCC, it is very likely that there is a substantial anthropogenic contribution to the global mean SLR since the 1970s, which is expected to continue during the 21st century. The main contributions to SLR come from ocean thermal expansion due to warming, from the Greenland and Antarctic ice sheets and land water storage. Since PA amplifies global temperature rise in the high latitude regions, we could have a substantial contribution of PA, above and beyond the contribution of global temperature rise, to SLR.

It is natural, therefore, to link SLR with global warming and in particular with PA, since some of the major contributions to SLR come from the Poles. As mentioned earlier, scientific evidence Bekryaev et al. (2010), IPCC (2013) suggests that the high latitude increase in temperature is *approximately twice* the estimates for the average global mean (IPCC, 2013; Winton, 2006). In terms of modeling SLR in the economics of climate change, the 2010RICE contains a module that projects future SLR with a set of linear relationships.²⁹ Although it is beyond the scope of this paper to model SLR, we will use a very simple approach based on 2010RICE to indicate whether ignoring PA, and calculating SLR damages using the global average temperature, makes a difference.

Assume a simple linear relationship between changes in SLR from a base level and temperature in box 2, $\Delta SLR \sim \Delta T_2$, where ΔT_2 denotes change in temperature in box 2. For the relation to be accurate, ζ must be adjusted to separate the ocean thermal warming from the ice sheets and glaciers and small ice caps effects as in 2010RICE. Boettle et al. (2016) propose a power law for damages associated with floods due to SLR, of the form $d_2 \sim (\Delta SLR)^\gamma$ with $\gamma > 1$. Actually, in case studies for Copenhagen and Kalundborg, γ was estimated to be 1.6 and 4.1 respectively. These estimates of the parameter γ suggest that SLR damages increase faster than SLR itself. Using the linear relationship between SLR and temperature, we can approximate d_2 , by $d_2 \sim (\Delta T_2)^\gamma$. If instead of ΔT_2 we use the change in global temperature, which is lower than ΔT_2 by a factor of approximately 1/2, we underestimate damages by a factor of $(1/2)^\gamma$. This suggests that d_2 could be high relative to the case where PA is ignored and potentially high relative to d_1 .³⁰

To summarize, the discussion above suggests that marginal damages from an increase in average global temperature are likely to be higher in box 1 relative to box 2, while damages from an increase in temperature in box 2 that does not include the PA effect could result in underestimation of these marginal damages. This discussion also suggests that, if heat transport phenomena and PA are introduced into the economics of climate change, future research is required to provide reliable estimates of damages emerging from temperature changes in different regions, or boxes.

In view of the above we consider the case of strong PA effects on marginal damages and perform our simulations for $d_1 \in [0.01, 0.1]$, $d_2 \in [0.1, 0.2]$. For the rest of the parameters, we use $L(1) = L(2) = 3.23$ billion,³¹ $\alpha = 0.05$, $\rho = 0.02$. Finally, we assume equal welfare weights between the two regions, $\nu(1) = \nu(2) = 1$.

References

- ACIA, 2004. Impacts of a Warming Arctic: Arctic Climate Impact Assessment. Cambridge University Press, Cambridge.
- Alexeev, V.A., 2003. Sensitivity to CO₂ doubling of an atmospheric GCM coupled to an oceanic mixed layer: a linear analysis. *Clim. Dyn.* 20, 775–787.
- Alexeev, V.A., Jackson, C.H., 2013. Polar amplification: is atmospheric heat transport important? *Clim. Dyn.* 41, 533–547. doi:10.1007/s00382-012-1601-z.
- Alexeev, V.A., Jackson, C.H., 2013. Erratum to: polar amplification: is atmospheric heat transport important? *Clim. Dyn.* 41 (2). doi:10.1007/s00382-013-1763-3.
- Alexeev, V.A., Langen, P.L., Bates, J.R., 2005. Polar amplification of surface warming on an aquaplanet in “ghost forcing” experiments without sea ice feedbacks. *Clim. Dyn.* 24 (2), 655–666. doi:10.1007/s00382-005-0018-3.
- Arrhenius, S., 1897. On the influence of carbonic acid in the air upon the temperature of the ground. *Publ. Astron. Soc. Pac.* 9 (54), 14.
- Athanassoglou, S., Xepapadeas, A., 2012. Pollution control with uncertain stock dynamics: when, and how, to be precautionous. *J. Environ. Econ. Manag.* 63, 304–320.
- Bekryaev, R., Polyakov, I., Alexeev, V., 2010. Role of polar amplification in long-term surface air temperature variations and modern arctic warming. *J. Clim.* 23, 3888–3906.
- Belaia, M., Funke, M., Glanemann, N., 2015. Global warming and a potential tipping point in the atlantic thermohaline circulation: the role of risk aversion. *Environ. Resour. Econ.* doi:10.1007/s10640-015-9978-x.
- Boettle, M., Rybski, D., Kropp, J.P., 2016. Quantifying the effect of sea level rise and flood defence – a point process perspective on coastal flood damage. *Nat. Hazards Earth Syst. Sci.* 16, 559–576.
- Borgerson, S., 2008. Arctic meltdown: the economic and security implications of global warming. *Foreign Aff.* 87 (2), 63–77.
- Bosello, F., Roson, R.R., Tol, R., 2007. Economy-wide estimates of the implications of climate change: sea level rise. *Environ. Resour. Econ.* 37, 549–571.

²⁹ See http://www.econ.yale.edu/~nordhaus/homepage/documents/SLR_02190RICE, and Bosello et al. (2007) for regional estimates of SLR damages based on regional land and capital losses due to SLR of 1m. These estimates are not, however, helpful in calibrating d_2 , since there is no clear link to PA.

³⁰ Furthermore results presented by Ceronsky et al. (2011) suggest that heat transport from the lower box to the upper box magnified by PA should incrementally increase the probability of events like the Greenland ice sheet melt, which in turn increase the damages due to increased flooding to poor areas in the lower box where land is cheaper due to flooding risk. This argument suggests that the parameter d_{12} is likely to be relatively large.

³¹ Evidence suggests that roughly 88% of the global population of 7.347 billion in 2015 (World Bank, <http://data.worldbank.org/indicator/SP.POP.TOTL>), lives in the northern hemisphere, and about half lives north of 27° N (<http://www.radicalcartography.net/index.html?histpop>).

- Brock, W., Engström, G., Grass, D., Xepapadeas, A., 2013. Energy balance climate models and general equilibrium optimal mitigation policies. *J. Econ. Dyn. Control* 37 (12), 2371–2396.
- Brock, W., Engström, G., Xepapadeas, A., 2014. Energy balance climate models, damage reservoirs, and the time profile of climate change policy. In: Bernard, L., Semmler, W. (Eds.), *The Oxford Handbook of the Macroeconomics of Global Warming*. Oxford University Press, Oxford, chapter 3.
- Brock, W., Engström, G., Xepapadeas, A., 2014. Spatial climate economic models in the design of optimal climate policies across locations. *Eur. Econ. Rev.* 69, 78–103.
- Cai, Y., Brock, W., Xepapadeas, A., 2017. Climate change economics and heat transport across the globe: Spatial-DSICE. Proceedings of the 2017 Allied Social Science Association (ASSA) Annual Meeting Chicago, <http://purl.umcn.edu/251833>.
- Cai, Y., Judd, K.L., Lenton, T.M., Lontzek, T.S., Narita, D., 2015. Environmental tipping points significantly affect the cost-benefit assessment of climate policies. *PNAS* 112 (15), 4606–4611.
- Cai, Y., Judd, K. L., Lontzek, T. S., 2015a. The social cost of carbon with economic and climate risks. Papers 1504.06909, arXiv.org, revised Apr 2015.
- Ceronsky, M., Anthoff, D., Hepburn, C., Tol, R., 2011. Checking the Price Tag on Catastrophe: The Social Cost of Carbon Under Non-linear Climate Response. Working Paper no. 392, ESRI.
- D'Autume, A., Schubert, K., Withagen, C., 2016. Should the carbon price be the same in all countries. *J. Public Econ. Theory* 18 (5), 709–725.
- Dietz, S., Stern, N., 2015. Endogenous growth, convexity of damage and climate risk: how Nordhaus' framework supports deep cuts in carbon emissions. *Econ. J.* 125 (583), 547–620.
- Fanning, A., Weaver, A., 1996. An atmospheric energy moisture-balance model: climatology, interpentadal climate change and coupling to an OGCM. *J. Geophys. Res.* 101 (15), 111–115.
- Francis, J., Skific, N., 2015. Evidence linking rapid arctic warming to mid-latitude weather patterns. *Philos. Trans. R. Soc. A* 373. dx.doi.org/10.1098/rsta.2014.0170
- Francis, J., Vavrus, S., 2014. Evidence for a wavier jet stream in response to rapid arctic warming. *Environ. Res. Lett.* 10, 1–12.
- Gerlagh, R., Liski, M., 2016. Carbon prices for the next hundred years. *Econ. J.* doi:10.1111/eoj.12436.
- Golosov, M., Hassler, J., Krusell, P., Tsyvinski, A., 2014. Optimal taxes on fossil fuel in equilibrium. *Econometrica* 82 (1), 41–88.
- Graversen, R.G., Wang, M., 2009. Polar amplification in a coupled climate model with locked albedo. *Clim. Dyn.* 33, 629–643.
- Hansen, L., Sargent, T., 2008. *Robustness in Economic Dynamics*. Princeton University Press, Princeton.
- Holland, M.M., Bitz, C.M., 2003. Polar amplification of climate change in coupled models. *Clim. Dyn.* 21, 221–232.
- IPCC, 2013. *Climate Change 2013, The Physical, Science Basis*. Cambridge University Press, New York.
- Jensen, S., Traeger, C., 2014. Optimal climate change mitigation under long-term growth uncertainty: stochastic integrated assessment and analytic findings. *Eur. Econ. Rev.* 69, 104–125.
- Knutti, R., 2013. Relationship between global emissions and global temperature rise. *Climate Change 2013, The Physical, Science Basis, IPCC. CLA chapter 12*.
- Kug, J.-S., Jeong, J.H., Jang, Y.-S., Kim, B.-M., Folland, C.K., Min, S.-K., Son, S.-W., 2015. Two distinct influences of arctic warming on cold winters over north america and east asia. *Nat. Geosci.* 8, 759–762. doi:10.1038/ngeo2517.
- Langen, P.L., Alexeev, V.A., 2007. Polar amplification as a preferred response in an idealized aquaplanet GCM. *Clim. Dyn.* 29, 305–317. doi:10.1007/s00382-006-0221-x.
- Leduc, M., Matthews, H.D., de Elía, R., 2015. Quantifying the limits of a linear temperature response to cumulative CO₂ emissions. *J. Clim.* 28 (24), 9955–9968.
- Leduc, M., Matthews, H.D., de Elía, R., 2016. Regional estimates of the transient climate response to cumulative CO₂ emissions. *Nat. Clim. Change* 6, 474–478.
- Lenton, T., n.d. earthsystem tipping points. Available at [https://yosemite.epa.gov/ee/epa/erm.nsf/vwAN/EE-0564-112.pdf/\\$file/EE-0564-112.pdf](https://yosemite.epa.gov/ee/epa/erm.nsf/vwAN/EE-0564-112.pdf/$file/EE-0564-112.pdf).
- Lenton, T., Held, H., Kriegler, E., Hall, J., Lucht, W., Rahmstorf, S., Schellnhuber, H.J., 2008. Tipping elements in the Earth's climate system. *PNAS* 105 (6), 1786–1793.
- MacDougall, A.H., Friedlingstein, P., 2015. The origin and limits of the near proportionality between climate warming and cumulative CO₂ emissions. *J. Clim.* 28, 4217–4230.
- Masson-Delmotte, V., Kageyama, M., Braconnot, P., Charbit, S., Krinner, G., Ritz, C., Guilyardi, E., Jouzel, J., Abe-Ouchi, A., Crucifix, M., Gladstone, R.M., Hewitt, C.D., Kitoh, A., LeGrande, A.N., Marti, O., Merkel, U., Motoi, T., Ohgaito, R., Otto-Bliesner, B., Peltier, W.R., Ross, I., Valdes, P.J., Vittoretti, G., Weber, S.L., Wolk, F., Yu, Y., 2006. Past and future polar amplification of climate change: climate model intercomparisons and icecore constraints. *Clim. Dyn.* 26, 513–529.
- Matthews, H. D., Gillett, N. P., Stott, P. A., Zickfeld, K., 2009. The proportionality of global warming to cumulative carbon emissions. *Nature*, 459, 829–833.
- Matthews, H.D., Solomon, S., Pierrehumbert, R., 2012. Cumulative carbon as a policy framework for achieving climate stabilization. *Philos. Trans. R. Soc. A* 370, 4365–4379.
- Mendelsohn, R.O., 2009. The impact of climate change on agriculture in developing countries. *J. Nat. Resour. Policy Res.* 1 (1), 5–19.
- Moyer, E.J., Woolley, M.D., Matteson, N.J., Glotter, M.J., Weisbach, D.A., 2014. Climate impacts on economic growth as drivers of uncertainty in the social cost of carbon. *J. Legal Stud.* 43 (2), 401–425.
- Nordhaus, W., Sator, P., 2013. DICE 2013R: Introduction and User's Manual. Yale University Technical report.
- Nordhaus, W.D., 2007. *A Question of Balance: Weighing the Options on Global Warming Policies*. Yale University Press, New Haven, CT.
- Parry, I., Veung, C., Heine, D., 2014. How Much Carbon Pricing is in Countries' Own Interests? The Critical Role of Co-Benefits. Working Paper, WP/14/74 IMF.
- Pithan, F., Mauritsen, T., 2014. Arctic amplification dominated by temperature feedbacks in contemporary climate models. *Nat. Geosci. Lett.* 7, 181–184. doi:10.1038/NNGEO2071.
- Rahmstorf, S., Coumou, D., 2011. Increase of extreme events in a warming world. In: Proceedings of the 2011 National Academy of Sciences of the USA 108 doi:10.1073/pnas.1101766108.
- Schaefer, K., Lantuit, H., Romanovsky, V.E., Schuur, E.A.G., Witt, R., 2014. The impact of the permafrost carbon feedback on global climate. *Environ. Res. Lett.* 9, 1–9. doi:10.1088/1748-9326/9/8/085003.
- Schuur, E.A.G., McGuire, A.D., Schadel, C., Grosse, G., Harden, J.W., Hayes, D.J., Hugelius, G., Koven, C.D., Kuhry, P., Lawrence, D.M., Natali, S.M., Olefeldt, D., Romanovsky, V.E., Schaefer, K., Turetsky, M.R., Treat, C.C., Vonk, J.E., 2015. Climate change and the permafrost carbon feedback. *Nature* 520, 171–179.
- Screen, J.A., Simmonds, I., 2014. Amplified mid-latitude planetary waves favor particular regional weather extremes. *Nat. Clim. Change* 4, 704–709. doi:10.1038/nclimate2271.
- Serreze, M., Barry, R., 2011. Processes and impacts of arctic amplification: a research synthesis. *Glob. Planet. Change* 77, 85–96.
- Stroeve, J., Holland, M.M., Meier, W., Scambos, T., Serreze, M.C., 2007. Arctic sea ice decline: faster than forecast. *Geophys. Res. Lett.* 34, L09501. doi:10.1029/2007GL029703.
- Tarnocai, C., Canadell, J., Schuur, E., Kuhry, P., Mazhitova, G., Zimov, S., 2009. Soil organic carbon pools in the northern circumpolar permafrost region. *Glob. Biogeochem. Cycles* 23 (2), GB2023.
- Thomas, D.S., Twyman, C., 2005. Equity and justice in climate change adaptation amongst natural-resource-dependent societies. *Glob. Environ. Change* 15, 115–124.
- van der Ploeg, F., Rezaei, A., 2016. Cumulative emissions, unburnable fossil fuel, and the optimal carbon tax. *Technol. Forecast. Soc. Change*. <http://dx.doi.org/10.1016/j.techfore.2016.10.016>.
- Wagner, T., Eisenman, I., 2015. How climate model complexity influences sea ice stability. *J. Clim.*, 28, 15 May, 2015, 3998–4014.
- Weaver, A.J., Eby, M., Wiebe, E.C., Bitz, C.M., Duffy, P.B., Ewen, T.L., Fanning, A.F., Holland, M.M., MacFadyen, A., Matthews, H.D., 2001. The UVic earth system climate model: model description, climatology, and applications to past, present and future climates. *Atmos. Ocean* 39 (4), 361–428.

- Weitzman, M.L., 2010. What is the “damages function” for global warming – and what difference might it make? *Clim. Change Econ.* 1 (1), 57–69.
- Winton, M., 2006. Amplified arctic climate change: what does surface albedo feedback have to do with it? *Geophys. Res. Lett.* 33, L03701. doi:10.1029/2005GL025244.
- Zachos, J.C., Pagani, M., Sloan, L.C., Thomas, E., Billups, K., 2001. Trends, rhythms and aberrations in global climate 65 ma to present. *Science* 292, 686–693.
- Zhang, T., Barry, R., Knowles, K., Ling, F., Armstrong, R., 2003. Distribution of seasonally and perennially frozen ground in the northern hemisphere. In: *Proceedings of the Eighth International Conference on Permafrost*. Zurich, Switzerland, pp. 1289–1294. 21–25 July 2003.
- Zickfeld, K., Bruckner, T., 2008. Reducing the risk of atlantic thermohaline circulation collapse: sensitivity analysis of emissions corridors. *Clim. Change* 91 (3), 291–315.
- Zickfeld, K., Slawig, T., Rahmstorf, S., 2004. A low-order model for the response of the atlantic thermohaline circulation to climate change. *Ocean Dyn.* 54, 8–26.